THE ANALOGY BETWEEN SURFACE SHOCK WAVES IN A LIQUID

AND SHOCKS IN COMPRESSIBLE GASES

Thesis by

Harry Eastwood Crossley, Jr.

In Partial Fulfillment of the Requirements

For the Degree of

Mechanical Engineer

California Institute of Technology

Pasadena, California

1950

ACKNOWLEDGMENTS

ABSTRACT

It has been known for some time that an analogy exists between the flow of a liquid with a free surface and the flow of a compressible gas. A less accurate analogy has been shown to obtain between hydraulic jumps and compression shocks. The interaction of shocks can occur in two forms, the regular or two-shock configuration and the Mach or three-shock configuration. The latter configuration is not yet completely understood, either in the case of hydraulic jumps in a free-surface liquid or in the case of shocks in a compressible gas. This experimental study was primarily concerned with the Mach interactions of hydraulic jumps. The conclusions of this study are: (a) there is a definite disagreement between experiment and existing theory; (b) a depth discontinuity, or wave, rather than a velocity discontinuity separates the region behind the Mach wave from the region behind the reflected wave; (c) there is evidence that, for interactions of weak hydraulic jumps, there is a deviation from constant depth between waves; (d) the Mach wave is convex for the interaction of the stronger hydraulic jumps, but is concave for the interaction of weak hydraulic jumps; (e) measurements should not be made so as to allow for curvature of the Mach without considering the curvature of the incident and reflected waves in the neighborhood of the triple point.

TABLE OF CONTENTS

LIST OF TABLES

LIST OF ILLUSTRATIONS

TABLE OF SYMBOLS

C	Celerity of Shock Wave Propagation.
c_p	Specific Heat at Constant Pressure of a Gas.
E	Internal Energy.
g	Conversion Factor in Newton's Law of Motion.
h	Depth of Free-surface Liquid.
M	Mach Number.
p	Pressure.
S	Designating a Shock Wave.
T	Absolute Temperature.
u	Velocity.
x,y,z	Cartesian Coordinates.
α	Half Angle between Incident Shock Waves.
α'	Half Angle between Reflected Shock Waves.
γ	Ratio of Specific Heats of a Gas.
δ	Half Angle between Directions of Motion of Triple Points of Mach Interaction.
ϵ	Half Angle between Lines of Velocity Discontinuity of Mach Interaction.
η	Ratio of Depth Following to Depth Preceding Incident Hydraulic Jump.
η'	Ratio of Depth Following to Depth Preceding Reflected Hydraulic Jump.
ξ	Pressure Ratio across Incident Shock Wave: Square of Depth Ratio across Incident Hydraulic Jump.

ξ' Pressure Ratio across Reflected Shock Wave: Square of Depth Ratio across Reflected Hydraulic Jump.

ρ Density

ω Angle between Incident Shock Wave and Direction of Motion of Triple Point of Mach Interaction.

ω' Angle between Reflected Shock Wave and Direction of Motion of Triple Point of Mach Interaction.

I INTRODUCTION

The flow of liquids with a free surface is of two different types: relatively smooth low-velocity flow, and high-velocity flow characterized by standing waves and sudden changes in depth known as hydraulic jumps.

The similarity between low-velocity free-surface flow and sub-sonic compressible gas flow, and between high-velocity free-surface flow and supersonic compressible gas flow, was first presented in mathematical form for two-dimensional motion by Jouget[1]* and for three-dimensional motion by Riabouchinsky.[2] Further investigations were made by Ippen,[3] Binnie and Hooker,[4] and von Karman.[5]

Preiswerk[6] investigated the extent of the analogy and applied the methods of the theory of compressible flow directly to the solution of problems in the field of liquid flow. More recent work consists of numerical flow calculations[7, 8] and a theoretical paper on liquid free-surface flow by Stoker,[9] with an appendix by Friedrichs.[10]

A comprehensive treatment of the analogy was given by Gilmore,[11] who derives the mathematical analogy in a manner somewhat simpler and more general than that used by Preiswerk, discusses the divergence of theory from the actual situation, and treats the application of the analogy to shock-intersection problems.

Some experimental verifications of the theory were included by

---

* Numbers in parentheses refer to references at end of this thesis.

Preiswerk[6] but most later work has been concerned with the practical application of the analogy to model testing[12, 13] Investigations have been made concerning the experimental reflection of shock waves in compressible flow[14, 15, 16] and studies have been made on the similar problem of hydraulic-jump intersections[17, 18]

The Mach reflection, or three-shock configuration, is not yet completely understood, either in the case of hydraulic jumps in a free-surface liquid or in the case of shocks in a compressible gas. It is experimentally simpler to study hydraulic-jump interactions, and it is possible that if sufficient information could be obtained to clarify this phenomenon, the interaction of shocks in compressible gases would also be more exactly understood.

The purpose of the experimental work herein reported is to study the interactions of hydraulic jumps, or surface shock waves in shallow liquids, especially Mach-type or three-shock interactions, and to attempt to ascertain the source of the discrepancy between experiment and theory.

II   DISCUSSION OF THEORY

The analogy between isentropic free-surface liquid flow and isentropic perfect-gas flow, and the analogy between hydraulic jumps and compression shocks, are presented here by the method developed by Gilmore.[11]   The quantitative relations for regular (two-shock) and Mach-type (three-shock) intersections follow the development by Einstein and Baird.[17, 18]

THE ISENTROPIC ANALOGY

Consider in the fluid a stream tube of infinitesimal cross section over which the fluid velocity, u, pressure, p, and other parameters are sensibly constant. If steady flow is assumed, with no viscous or thermal transfer of energy across the tube boundaries, the energy equation obtains:

$$E + \frac{p}{\rho} + \frac{1}{2}u^2 + gz = \text{constant} \tag{1}$$

where E corresponds to internal energy; p/ρ, to mechanical work; $\frac{1}{2}u^2$, to kinetic energy; and gz, to gravitational potential energy.

In a flow field where there are no viscous forces and the density is a constant or a function of pressure only, then (for proof see Ref. 19, pp. 112-116)

$$\int_{S'} \text{curl } \underline{u} \cdot d\underline{S}' = \text{constant} \tag{2}$$

where the surface S' is any surface fixed physically in the field, and the vorticity is a vector defined by

$$\text{curl } \underline{u} = \left[\frac{\partial u_z}{\partial y} - \frac{\partial u_y}{\partial z}\right]\underline{i} + \left[\frac{\partial u_x}{\partial z} - \frac{\partial u_z}{\partial x}\right]\underline{j} + \left[\frac{\partial u_y}{\partial x} - \frac{\partial u_x}{\partial y}\right]\underline{k} \qquad (3)$$

To apply the above equations to the flow of a liquid having a free surface and bounded below by a horizontal bed, the following simplifying assumptions are made: (a) constant liquid density; (b) constant pressure on the free surface; (c) surface tension forces negligible; (d) vertical acceleration of liquid negligible compared with the acceleration of gravity; (e) slope of free surface, considered in direction of fluid motion, of order ϵ; (f) boundary conditions independent of z. Eqs. (1), (2) and (3) then simplify to (Cf. Ref. 11)

$$\frac{1}{h}\left[\frac{\partial u_x}{\partial y} - \frac{\partial u_y}{\partial x}\right] = \text{constant} \qquad (4)$$

$$gh + \frac{1}{2}(u_x^2 + u_y^2) = \text{constant} \qquad (5)$$

The continuity equation for conservation of mass may be written

$$\frac{\partial}{\partial x}(hu_x) + \frac{\partial}{\partial y}(hu_y) = 0 \qquad (6)$$

The three equations (4), (5) and (6) for the three unknowns u_x, u_y (velocities) and h (liquid depth), together with appropriate boundary conditions, completely determine the liquid flow field.

In a perfect gas for which c_p is constant,

$$E + \frac{p}{\rho} = c_p T \qquad (7)$$

At ordinary temperatures and for distances up to a few hundred feet, gz is negligible compared to $c_p T$. Consider a two-dimensional gas flow, where all flow parameters and boundary conditions are indepen-

- 5 -

dent of z and $u_z = 0$. Equation (1) then becomes

$$c_p T + \frac{1}{2}(u_x^2 + u_y^2) = \text{constant} \tag{8}$$

The vorticity [Eq. (3)] has only a vertical component, and it can be shown that for a gas

$$\frac{1}{\rho}\left[\frac{\partial u_x}{\partial y} - \frac{\partial u_y}{\partial x}\right] = \text{constant} \tag{9}$$

The continuity equation is

$$\frac{\partial}{\partial x}(\rho u_x) + \frac{\partial}{\partial y}(\rho u_y) = 0 \tag{10}$$

In flow without viscous or thermal losses, the isentropic relation for a perfect gas holds:

$$p\,\rho^{-\gamma} = \text{constant} \quad \text{or} \quad \rho = T^{\frac{1}{\gamma-1}} \times \text{constant} \tag{11}$$

where γ is the ratio of specific heats for the gas. Substitution of Eq. (11) in Eqs. (9) and (10) yields, respectively,

$$T^{-\frac{1}{\gamma-1}}\left[\frac{\partial u_x}{\partial y} - \frac{\partial u_y}{\partial x}\right] = \text{constant} \tag{12}$$

$$\frac{\partial}{\partial x}(u_x T^{\frac{1}{\gamma-1}}) + \frac{\partial}{\partial y}(u_y T^{\frac{1}{\gamma-1}}) = 0 \tag{13}$$

The three equations (8), (12) and (13) for the three unknowns u_x, u_y (velocities) and T (absolute temperature), together with the appropriate boundary conditions, completely determine the gas flow.

The analogy between isentropic free-surface liquid flow and isentropic perfect-gas flow can be shown by a comparison of Eqs. (4), (5) and (6) with Eqs. (8), (12) and (13). Eq. (5) is equivalent to Eq. (8) if gh is replaced by $c_p T$. Eq. (4) is equivalent to Eq. (12) and Eq. (6) to Eq. (13) if two conditions are met:

$$gh \longleftrightarrow c_p T \qquad\qquad \text{and} \qquad\qquad \gamma = 2 \qquad\qquad (14)$$

The analogy between the motion of a free-surface liquid and a gas having $\gamma = 2$ is evidently complete within the limits of the assumptions made in deriving the flow equations, provided the boundary conditions are analogous.

According to dimensional arguments, similarity between two different physical situations must occur if all the corresponding dimensionless ratios of the relevant parameters are equal. Eq. (14) can therefore be written

$$\frac{h}{h_o} \longleftrightarrow \frac{T}{T_o} \qquad\qquad (\gamma = 2) \qquad\qquad (15)$$

where h_o and T_o are the height and temperature at some reference point. Also, according to Eq. (11),

$$\frac{h}{h_o} \longleftrightarrow \frac{\rho}{\rho_o} \qquad\qquad \text{and} \qquad\qquad \frac{h^2}{h_o^2} \longleftrightarrow \frac{p}{p_o} \qquad (\gamma = 2) \quad (16)$$

HYDRAULIC JUMPS AND COMPRESSION SHOCKS

A hydraulic jump is a steady elevation wave of finite amplitude produced by a sudden disturbance of the surface of a liquid or by an obstacle placed in a rapidly flowing liquid.

Consider a normal hydraulic jump occurring in a region of uniform parallel flow. The problem is reduced to one of steady flow by choosing coordinates stationary with respect to the jump. Let the fluid be flowing with height h_1 and uniform velocity u_1 up to the plane where the jump starts, and assume that at the plane a distance w behind the start of the jump the flow has a height h_2 and uniform

velocity u_2. The energy balance for steady flow [Eq. (1)], gives

$$E_1 + gh_1 + \frac{1}{2}u_1^2 = E_2 + gh_2 + \frac{1}{2}u_2^2 \tag{17}$$

The continuity relation is simply

$$h_1 u_1 = h_2 u_2 \tag{18}$$

The momentum equation can be written

$$\frac{1}{2}gh_1^2 + h_1 u_1^2 = \frac{1}{2}gh_2^2 + h_2 u_2^2 \tag{19}$$

Since Eqs. (18) and (19) do not involve internal energy E, they can be combined to yield

$$u_1 = \sqrt{\frac{gh_1}{2}(1 + \frac{h_2}{h_1})\frac{h_2}{h_1}} \tag{20}$$

By considering coordinates fixed with respect to the fluid ahead of the jump, it is seen that u_1 is the velocity with which a hydraulic jump will move into a still body of liquid.

To treat an oblique hydraulic jump, coordinates are chosen which move with the constant velocity u_p parallel to the jump. In such a coordinate system, the fluid ahead of the jump will appear to be moving into it at right angles, as in a normal jump. Since the equations of mechanics are invariant to such a coordinate transformation, the equations of a normal hydraulic jump in these coordinates are applicable. The results may be referred back to stationary coordinates simply by adding the uniform velocity u_p.

Consider a compression shock in a region of uniform parallel flow. Choose coordinates to make the shock stationary and normal to the flow: the conservation of energy Eq. (8) becomes

$$c_p T_1 + \frac{1}{2} u_1^2 = c_p T_2 + \frac{1}{2} u_2^2 \qquad (21)$$

The continuity relation Eq. (10) is

$$\rho_1 u_1 = \rho_2 u_2 \qquad (22)$$

The momentum equation is

$$p_1 + \rho_1 u_1^2 = p_2 + \rho_2 u_2^2 \qquad (23)$$

Equations (21), (22) and (23) are the Rankine-Hugoniot equations for a shock wave. Combined with the perfect gas relation

$$p = R \rho T = \frac{\gamma - 1}{\gamma} c_p \rho T \qquad (24)$$

they can be solved for any four of the variables, such as p_2, ρ_2, T_2 and u_2.

An analogy between hydraulic jumps and compression shocks can be found by comparing the basic equations for the two cases. The continuity conditions, Eqs. (18) and (22), are identical if h is taken to be equivalent to ρ. The two momentum relations, Eqs. (19) and (23), are equivalent if h corresponds to ρ and h^2 to $2p/g$. In order for this to be possible, ρ^2 and p must be proportional in the shock wave case, i.e.

$$\left(\frac{\rho_1}{\rho_2}\right)^2 \left(\frac{p_2}{p_1}\right) = 1 \qquad (25)$$

Using the shock-wave equations, with $\gamma = 2$,

$$\left(\frac{\rho_1}{\rho_2}\right)^2 \left(\frac{p_2}{p_1}\right) = 1 + \frac{4}{27}(M_1^2 - 1)^3 + \dots \qquad (\gamma = 2) \qquad (26)$$

Where M_1 is the initial Mach number, defined by

$$M_1 = \frac{u_1}{\sqrt{(\gamma - 1)c_p T_1}} \qquad (27)$$

Thus Eq. (25) is satisfied and the analogy is quite good for weak

shocks with $(M_1^2 - 1) \ll 1$, but for strong shocks it becomes increasingly inaccurate. Condition (25) is identical with the isentropic condition, Eq. (11), when $\gamma = 2$. Therefore, real hydraulic jumps (with losses) are analogous to fictitious isentropic compression shocks (without losses) in a gas having $\gamma = 2$.

THE REGULAR (TWO-SHOCK) INTERSECTION

For the intersection of two hydraulic jumps of equal strength, the line of symmetry is a streamline and can therefore be replaced by a wall if boundary friction is assumed negligible. The following theory is thus applicable to the reflection of a hydraulic jump from a rigid wall.

Consider the configuration shown in Fig. 1. The line of symmetry is taken as the x-axis; the incident wave S_1 is moving into stationary liquid. Area I is a region undisturbed by any wave; area II is the region through which the incident wave has passed; area III is the region through which both the incident and reflected waves have passed.

The velocity of propagation of the incident wave S_1 into the undisturbed liquid of area I is, from Eq. (20),

$$C_1 = \sqrt{\frac{gh_1}{2}(1 + \frac{h_2}{h_1})\frac{h_2}{h_1}} \tag{28}$$

If h_2 is assumed constant, the flow represented by the hydraulic jump superimposed on a body of still liquid and the general flow after the wave has passed must be equal. The continuity relationship can be written

$$u_2 h_2 = C_1 (h_2 - h_1) \tag{29}$$

The velocity u_2 can be resolved into components normal and parallel to the reflected wave S_2. From the geometry of Fig. 1, these components are

$$u_{2N} = u_2 \cos(\pi - \alpha - \alpha') = -u_2 \cos(\alpha + \alpha')$$
$$u_{2P} = u_2 \sin(\pi - \alpha - \alpha') = u_2 \sin(\alpha + \alpha') \tag{30}$$

Solve Eq. (29) for u_2 and substitute in Eq. (30):

$$u_{2N} = -C_1 (1 - \frac{h_1}{h_2}) \cos(\alpha + \alpha') \tag{31}$$

$$u_{2P} = C_1 (1 - \frac{h_1}{h_2}) \sin(\alpha + \alpha') \tag{32}$$

The velocity of the point of intersection along the line of symmetry must be the same for both waves; therefore,

$$\frac{C_1}{\sin \alpha} = \frac{C_2}{\sin \alpha'} \tag{33}$$

If h_3 is assumed constant, the general flow in area III normal to wave S_2 must be equal to the component of the flow in area II normal to S_2 plus the added flow due to S_2 superimposed on h_2. This continuity relation is written

$$u_{3N} h_3 = u_{2N} h_2 + C_2 (h_3 - h_2) \tag{34}$$

The components of u_2 and u_3 parallel to the wave S_2 must be equal;

$$u_{3P} = u_{2P} \tag{35}$$

The velocity of propagation of the reflected wave S_2 will be equal to the velocity of a similar wave in still water plus the normal component of the velocity in area II:

$$C_2 = u_{2N} + \sqrt{\frac{gh_2}{2} (1 + \frac{h_3}{h_2}) \frac{h_3}{h_2}} \tag{36}$$

Combine Eqs. (28), (31), (33) and (36):

$$\sqrt{\frac{gh_2}{2}(1 + \frac{h_3}{h_2})\frac{h_3}{h_2}} = \sqrt{\frac{gh_1}{2}(1 + \frac{h_2}{h_1})\frac{h_2}{h_1}} \left[\frac{\sin \alpha'}{\sin \alpha} + (1 - \frac{h_1}{h_2})\cos(\alpha + \alpha')\right] \quad (37)$$

Square both sides and simplify to

$$(\frac{h_3}{h_2})^2 + (\frac{h_3}{h_2}) - (1 + \frac{h_2}{h_1})\left[\frac{\sin \alpha'}{\sin \alpha} + (1 - \frac{h_1}{h_2})\cos(\alpha + \alpha')\right]^2 = 0 \quad (38)$$

This is a quadratic equation in h_3/h_2 for which the solutions are

$$\frac{h_3}{h_2} = -\frac{1}{2} \pm \left[\frac{1}{4} + (1 + \frac{h_2}{h_1})\left\{\frac{\sin \alpha'}{\sin \alpha} + (1 - \frac{h_1}{h_2})\cos(\alpha + \alpha')\right\}^2\right]^{\frac{1}{2}} \quad (39)$$

Since h_3/h_2 is always positive in the physical sense, only the plus sign before the radical need be considered.

If h_3 is assumed constant, the velocity u_3 must be parallel to the line of symmetry. Therefore, the component of u_3 normal to the line of symmetry must equal zero:

$$u_{3y} = u_{3N}\cos \alpha' - u_{3P}\sin \alpha' = 0 \quad (40)$$

with the convention that u_{3p} is positive when directed toward the intersection. Using Eqs. (31) through (35), Eq. (40) becomes

$$C_1\left[-\frac{h_2}{h_3}(1 - \frac{h_1}{h_2})\cos(\alpha + \alpha') + \frac{\sin \alpha'}{\sin \alpha}(1 - \frac{h_2}{h_3})\right]\cos \alpha'$$
$$- C_1(1 - \frac{h_1}{h_2})\sin(\alpha + \alpha')\sin \alpha' = 0 \quad (41)$$

Solve Eq. (41) for h_3/h_2:

$$\frac{h_3}{h_2} = \frac{\dfrac{\sin \alpha' \cos \alpha'}{\sin \alpha} + (1 - \frac{h_1}{h_2})\cos(\alpha + \alpha')\cos \alpha'}{\dfrac{\sin \alpha' \cos \alpha'}{\sin \alpha} - (1 - \frac{h_1}{h_2})\sin(\alpha + \alpha')\sin \alpha'} \quad (42)$$

Equation (42) may be simplified as follows:

$$\frac{h_3}{h_2} = \frac{\cos \alpha'\left[\sin \alpha' + (1 - \frac{h_1}{h_2})\cos(\alpha + \alpha')\sin \alpha\right]}{\sin \alpha'\left[\cos \alpha' - (1 - \frac{h_1}{h_2})\sin(\alpha + \alpha')\sin \alpha\right]}$$

$$= 1 + \frac{(1 - \frac{h_1}{h_2})\sin \alpha \cos \alpha}{\sin \alpha'\left[\cos \alpha' - (1 - \frac{h_1}{h_2})\sin(\alpha + \alpha')\sin \alpha\right]}$$

$$\frac{h_3}{h_2} = 1 - \frac{\cos \alpha}{\sin \alpha' \left[\sin(\alpha + \alpha') - \frac{1}{(1 - \frac{h'}{h_2})} \frac{\cos \alpha'}{\sin \alpha} \right]} \tag{43}$$

The strength ξ of a hydraulic jump is defined as

$$\xi = (\frac{h'}{h_2})^2 \tag{44}$$

since it is thus analagous to the pressure ratio across a compression shock in a gas. Letting

$$\xi' = (\frac{h_2}{h_3})^2 \tag{45}$$

and substituting Eqs. (44) and (45) in Eqs. (39) and (43), two equations are obtained involving the four variables α, α', ξ and ξ':

$$(\frac{1}{\xi'})^{\frac{1}{2}} = -\frac{1}{2} + \left[\frac{1}{4} + (1 + \frac{1}{\xi^{\frac{1}{2}}}) \left\{ \frac{\sin \alpha'}{\sin \alpha} + (1 - \xi^{\frac{1}{2}}) \cos(\alpha + \alpha') \right\}^2 \right]^{\frac{1}{2}} \tag{46}$$

$$(\frac{1}{\xi'})^{\frac{1}{2}} = 1 - \frac{\cos \alpha}{\sin \alpha' \left[\sin(\alpha + \alpha') - \frac{1}{(1 - \xi^{\frac{1}{2}})} \frac{\cos \alpha'}{\sin \alpha} \right]} \tag{47}$$

The characteristics of the intersection of two similar hydraulic jumps are completely determined if the values of ξ and α are known. If values of α' are assumed, the value for ξ' can be found from both Eq. (46) and Eq. (47). These two values of ξ' are plotted against α'; if the curves intersect, a regular interaction is possible and ξ' and α' are given by the common value of the two curves.

THE MACH (THREE-SHOCK) INTERSECTION

Consider the configuration shown in Fig. 2. The line of symmetry is taken as the x-axis; the incident wave is moving into sta-

tionary fluid. Four areas are involved as follows: area I through
which no wave has passed; area II through which only the incident
wave S_1 has passed; area III through which both wave S_1 and the re-
flected wave S_2 have passed; area IV through which only the Mach
wave S_3 has passed. The line I"I which separates areas III and IV
is indicated by S_4.

The fundamental assumptions are: (a) the three hydraulic jumps
are straight and the Mach is normal to the line of symmetry; (b) the
depths h_1, h_2 and h_3 are constant within the respective areas and
with respect to time.

The velocity of propagation of the incident wave S_1 into the
undisturbed liquid of area I is, from Eq. (20),

$$C_1 = \sqrt{\frac{gh_1}{2}(1 + \frac{h_2}{h_1})\frac{h_2}{h_1}} \tag{48}$$

The velocity of propagation of the Mach wave S_3 is

$$C_3 = \sqrt{\frac{gh_1}{2}(1 + \frac{h_3}{h_1})\frac{h_3}{h_1}} \tag{49}$$

since the depth h_4 is assumed equal to the depth h_3. The following
relations from the development of the regular intersection theory
are applicable to the three-shock configuration:

$$u_2 = C_1(1 - \frac{h_1}{h_2}) \tag{29}$$

$$u_{2N2} = -C_1(1 - \frac{h_1}{h_2})\cos(\alpha + \alpha') \tag{31}$$

$$u_{2P2} = C_1(1 - \frac{h_1}{h_2})\sin(\alpha + \alpha') \tag{32}$$

$$u_{3N2} = u_{2N2}\frac{h_2}{h_3} + C_2(1 - \frac{h_2}{h_3}) \tag{34}$$

$$u_{3P2} = u_{2P2} \tag{35}$$

$$C_2 = u_{2N2} + \sqrt{\frac{gh_2}{2}(1 + \frac{h_3}{h_2})\frac{h_3}{h_2}} \qquad (36)$$

The subscript 2N2 indicates the component velocity in area II normal to the wave S_2; 3P2, the component velocity in area III parallel to the wave S_2. A similar convention is used for other component velocities.

From the geometry of Fig. 2, with the convention that u_{3P2} is positive when directed toward the point of intersection I, the velocity in area III parallel to the line I"I is

$$u_{3P4} = u_{3N2} \sin(\alpha' + \epsilon) + u_{3P2} \cos(\alpha' + \epsilon) \qquad (50)$$

Similarly the velocity in area III normal to the line I"I is

$$u_{3N4} = u_{3P2} \sin(\alpha' + \epsilon) - u_{3N2} \cos(\alpha' + \epsilon) \qquad (51)$$

Combining Eqs. (32) and (35),

$$u_{3P2} = C_1(1 - \frac{h_1}{h_2})\sin(\alpha + \alpha') \qquad (52)$$

And from Eqs. (31), (34) and (36)

$$u_{3N2} = -C_1(1 - \frac{h_1}{h_2})\cos(\alpha + \alpha') + (1 - \frac{h_2}{h_3})\sqrt{\frac{gh_2}{2}(1 + \frac{h_3}{h_2})\frac{h_3}{h_2}} \qquad (53)$$

Substituting Eqs. (52) and (53) in Eq. (50):

$$\begin{aligned}
u_{3P4} = &-C_1(1 - \frac{h_1}{h_2})\cos(\alpha + \alpha')\sin(\alpha' + \epsilon) \\
&+ (1 - \frac{h_2}{h_3})\sqrt{\frac{gh_2}{2}(1 + \frac{h_3}{h_2})\frac{h_3}{h_2}}\sin(\alpha' + \epsilon) \\
&+ C_1(1 - \frac{h_1}{h_2})\sin(\alpha + \alpha')\cos(\alpha' + \epsilon) \\
= &\ C_1(1 - \frac{h_1}{h_2})\sin(\alpha - \epsilon) + (1 - \frac{h_2}{h_3})\sqrt{\frac{gh_2}{2}(1 + \frac{h_3}{h_2})\frac{h_3}{h_2}}\sin(\alpha' + \epsilon)
\end{aligned} \qquad (54)$$

Substituting Eqs. (52) and (53) in Eq. (51):

$$\begin{aligned}
u_{3N4} = &\ C_1(1 - \frac{h_1}{h_2})\cos(\alpha + \alpha')\cos(\alpha' + \epsilon) \\
&- (1 - \frac{h_2}{h_3})\sqrt{\frac{gh_2}{2}(1 + \frac{h_3}{h_2})\frac{h_3}{h_2}}\cos(\alpha' + \epsilon) \\
&+ C_1(1 - \frac{h_1}{h_2})\sin(\alpha + \alpha')\sin(\alpha' + \epsilon)
\end{aligned}$$

$$u_{3N4} = C_1 (1 - \frac{h_1}{h_2})\cos(\alpha - \epsilon) - (1 - \frac{h_2}{h_3})\sqrt{\frac{gh_2}{2}(1 + \frac{h_3}{h_2})\frac{h_3}{h_2}}\cos(\alpha' + \epsilon) \tag{55}$$

The flow represented by the hydraulic jump S_3 superimposed on the stationary liquid in area I and the general flow in area IV must be equal. The continuity relationship can be written

$$u_4 h_3 = C_3 (h_3 - h_1) \tag{56}$$

Then the velocity in area IV is given by

$$u_4 = C_3(1 - \frac{h_1}{h_3}) = (1 - \frac{h_1}{h_3})\sqrt{\frac{gh_1}{2}(1 + \frac{h_3}{h_1})\frac{h_3}{h_1}} \tag{57}$$

The component parallel to the line I"I is

$$u_{4P4} = u_4\cos\epsilon = (1 - \frac{h_1}{h_3})\sqrt{\frac{gh_1}{2}(1 + \frac{h_3}{h_1})\frac{h_3}{h_1}}\cos\epsilon \tag{58}$$

and the component normal to the line I"I is

$$u_{4N4} = u_4\sin\epsilon = (1 - \frac{h_1}{h_3})\sqrt{\frac{gh_1}{2}(1 + \frac{h_3}{h_1})\frac{h_3}{h_1}}\sin\epsilon \tag{59}$$

The triple point I of the intersection originates at I' and moves along I'I. During this time interval, however, the liquid through which this point has passed moves to a position along the line I"I due to the flow velocities. Therefore,

$$\frac{\tan\epsilon}{\tan\delta} = \frac{C_3}{C_3 - u_4} = \frac{C_3}{C_3 - C_3(1 - \frac{h_1}{h_3})} = \frac{h_3}{h_1}$$

$$\tan\delta = \frac{h_1}{h_3}\tan\epsilon \tag{60}$$

The intersection of the incident wave S_1 and the reflected wave S_2 moves along the line I'I; so,

$$\frac{C_1}{\sin(\alpha - \delta)} = \frac{C_2}{\sin(\alpha' + \delta)} \tag{61}$$

With the relations of Eqs. (31), (36) and (48), Eq. (61) becomes

$$\sqrt{\frac{gh_1}{2}(1 + \frac{h_2}{h_1})\frac{h_2}{h_1}}\sin(\alpha' + \delta) = \left[\sqrt{\frac{gh_2}{2}(1 + \frac{h_3}{h_2})\frac{h_3}{h_2}}\right.$$
$$\left. - (1 - \frac{h_1}{h_2})\sqrt{\frac{gh_1}{2}(1 + \frac{h_2}{h_1})\frac{h_2}{h_1}}\cos(\alpha + \alpha')\right]\sin(\alpha - \delta) \quad (62)$$

The intersection of the incident wave S_1 and the Mach wave S_3 also moves along the line $I'I$; then,

$$\frac{C_1}{\sin(\alpha - \delta)} = \frac{C_3}{\cos \delta} \quad (63)$$

Substituting Eqs. (48) and (49) in Eq. (63):

$$\sqrt{\frac{gh_1}{2}(1 + \frac{h_2}{h_1})\frac{h_2}{h_1}}\cos \delta = \sqrt{\frac{gh_1}{2}(1 + \frac{h_3}{h_1})\frac{h_3}{h_1}}\sin(\alpha - \delta) \quad (64)$$

For continuity, the velocities normal to the line $I''I$ must be the same and equal to the velocity of the line itself; thus,

$$u_{4N4} = u_{3N4} \quad (65)$$

Using the relations of Eqs. (48), (55) and (59), one gets for Eq.(65)

$$(1 - \frac{h_1}{h_3})\sqrt{\frac{gh_1}{2}(1 + \frac{h_3}{h_1})\frac{h_3}{h_1}}\sin \epsilon = (1 - \frac{h_1}{h_2})\sqrt{\frac{gh_1}{2}(1 + \frac{h_2}{h_1})\frac{h_2}{h_1}}\cos(\alpha - \epsilon)$$
$$- (1 - \frac{h_2}{h_3})\sqrt{\frac{gh_2}{2}(1 + \frac{h_3}{h_2})\frac{h_3}{h_2}}\cos(\alpha' + \epsilon) \quad (66)$$

Since the intersection of the reflected wave S_2 and the Mach wave S_3 also moves along the line $I'I$,

$$\frac{C_2}{\sin(\alpha' + \delta)} = \frac{C_3}{\cos \delta} \quad (67)$$

Combining Eqs. (31), (36), (48) and (49) with Eq. (67):

$$(1 - \frac{h_1}{h_3})\sqrt{\frac{gh_1}{2}(1 + \frac{h_3}{h_1})\frac{h_3}{h_1}}\sin(\alpha' + \delta) = \left[\sqrt{\frac{gh_2}{2}(1 + \frac{h_3}{h_2})\frac{h_3}{h_2}}\right.$$
$$\left. - (1 - \frac{h_1}{h_2})\sqrt{\frac{gh_1}{2}(1 + \frac{h_2}{h_1})\frac{h_2}{h_1}}\cos(\alpha + \alpha')\right]\cos \delta \quad (68)$$

Equation (68) involves the same variables as Eq. (62) and may be used as a substitute.

Because of the relation expressed by Eq. (65), the velocities parallel to the line I"I must not be equal. The line I"I thus represents a surface of velocity discontinuity, or slip plane. The slip velocity can be obtained from

$$u_s = u_{3P4} - u_{4P4} \tag{69}$$

with u_{3P4} and u_{4P4} given by Eqs. (54) and (58) respectively.

The introduction of the wave strengths defined by Eqs. (44) and (45) results in unnecessary complication; therefore, let

$$\eta = \left(\frac{1}{\xi}\right)^{\frac{1}{2}} = \frac{h_2}{h_1} \quad ; \qquad \eta' = \left(\frac{1}{\xi'}\right)^{\frac{1}{2}} = \frac{h_3}{h_2} \tag{70}$$

Upon substitution of Eq. (70) in Eqs. (60), (62), (64) and (66), four equations are obtained involving the six variables α, α', ϵ, δ, η and η':

$$\tan \epsilon = \eta \eta' \tan \delta \tag{71}$$

$$\eta'(1 + \eta') = (1 + \eta)\left[\frac{\sin(\alpha' + \delta)}{\sin(\alpha - \delta)} + \left(1 - \frac{1}{\eta}\right)\cos(\alpha + \alpha')\right]^2 \tag{72}$$

$$\eta'(1 + \eta \eta')\sin^2(\alpha - \delta) = (1 + \eta)\cos^2 \delta \tag{73}$$

$$\left(1 - \frac{1}{\eta \eta'}\right)\sqrt{1 + \eta \eta'} \sin \epsilon = \left(1 - \frac{1}{\eta}\right)\sqrt{1 + \eta} \cos(\alpha - \epsilon)$$
$$- \left(1 - \frac{1}{\eta'}\right)\sqrt{\eta'(1 + \eta')} \cos(\alpha' + \epsilon) \tag{74}$$

The characteristics of the intersection of two similar hydraulic jumps are completely determined if the values of α and ξ (thus η) are known.

The solutions for the regular and Mach intersections have been computed by Einstein and Baird[18] and are presented in graphical form in Figs. 3 and 4. For the regular intersections, the curves give the values computed from Eqs. (46) and (47). For the Mach

intersections the values are taken from tables prepared by the Mathematical Tables Project.[20]   These values are in essential agreement with the theory represented by Eqs. (71) through (74).

III   EXPERIMENTAL PROCEDURE

Hydraulic jumps, or surface shock waves, are produced by means of generators in a liquid such as water contained in a shallow ripple tank. Variations in water depth are measured by means of electrode pairs in conjunction with a recording oscillograph. Photograms of the waves are made directly on sensitized paper utilizing the light from a high voltage spark. A mechanical timer facilitates coordination of the electrically operated apparatus.

GENERATION OF HYDRAULIC JUMPS

The ripple tank consists of a shallow glass-bottom tank approximately five feet long and four feet wide. The tank is supported on a framework built as rigidly as necessary to prevent the creation of undesired waves by vibration of the frame (Fig. 5).

The liquid used in the ripple tank is a solution (0.001 to 0.002 normal) of manganous chloride in distilled water, the salt being added to give more uniform electrolytic characteristics when the electrical method of depth measurement is used. The liquid is stored in five-gallon glass bottles above the ripple tank: the transfer from tank to storage is accomplished by means of an aspirator.

The surface shock waves are produced by means of the apparatus shown in Fig. 6. The wave generator is 24 inches long and makes wave fronts of the same length. The reservoir into which the water is drawn prior to its release is 9 inches high and has a variable

cross-section as indicated in Fig. 6. Air inlet valves are located
at the quarter points of the top surface. These valves are opened
by springs tripped by electrical solenoids. The valve openings are
throttled by means of removable orifice plates. The water is made
to rise inside the generator by reducing the pressure by means of a
vacuum pump or aspirator. The face of the discharge slot is milled
from heavy brass tubing, thus providing for a uniform discharge
through the full length of the slot. The body of the generator can
be lifted by means of a rack and pinion to vary the height of the
discharge slot.

The following variables affect the strength of the generated
wave: (a) the general water level in the ripple tank; (b) the
height to which water is raised in the generator; (c) the diameter
of the air inlet orifice; (d) the height of the discharge slot.

The more important variables are the initial depth of the water
in the ripple tank and the air inlet diameter. Their effect upon
wave strength is indicated in Fig. 7. It is seen that a given wave
strength can be obtained by a suitable choice of initial water depth
and air inlet diameter.

In Fig. 8 is indicated the effect upon wave strength of generator
head, i.e. the height to which water is raised in the generator reser-
voir before release. In general the effect seems to be negligible
within experimental error for a generator head above 18 centimeters.

The height of the discharge slot has a negligible effect upon

wave strength. However, the height of the discharge slot is important, especially for strong waves, since, if the wave is created through too narrow a slot, the resulting effect is that of a jet of water overriding the still water.

The ability of the two available generators to create identical waves is within experimental error provided a generator head of 19 to 21 centimeters is used.

DEPTH MEASUREMENT

The depth of liquid at any point in the ripple tank is determined by means of a pair of electrodes. Three of these electrode pairs were used, each connected to one channel of a Consolidated Engineering Corporation recording oscillograph (Type 5-101 A) which enabled depth to be recorded as a function of time. A typical oscillogram is shown in Fig. 9.

The electrode pair consists of two platinum wires supported vertically so that the length of the wire immersed is equal to the depth of the liquid (Fig. 10). Since the separation is kept constant, any variation in the height of the liquid causes the resistance to vary in an inverse manner. The electrical system has been arranged so that this relationship is nearly linear.

A voltage of approximately three volts across the electrode terminals is produced by an oscillator giving an alternating current with a frequency of about 1000 cycles per second. This frequency is too high to be recorded by the low-frequency galvanometers of the

oscillograph.

The alternating current is used to minimize any electrolysis effects: with the voltage and frequency used, these effects are essentially reduced to zero.

An automatic current interrupter breaks the galvanometer circuit at intervals of approximately 0.6 second. The interruptions last for about 0.02 second. This results in a series of points which establish the zero displacement. This method eliminates any error due to drift of galvanometer.

The electrodes are calibrated by means of a point gage before and usually after a set of observations. The electrodes should be kept clean to obtain consistent calibrations. A satisfactory procedure is a periodic dip of the electrodes in concentrated nitric acid, ammonium hydroxide (two normal) and water, in that order, with a dip in carbon tetrachloride before each set of observations. It has been found that the oscillator output tends to drift in magnitude thus affecting calibration. If the oscillator is allowed to warm up for 1/2 to 3/4 hour before being used, the drift thereafter is very small.

If the preliminary calibration is plotted with oscillogram values as ordinate vs. point gage values as abscissa, the drift in oscillator output tends to change the slope of the linear portion of the calibration curve without affecting the intercept of the line extended and the vertical axis. This fact can be used to determine the

calibration for each observation. The initial water depth is measured by means of the point gage and plotted; a line through this point and the above mentioned intercept point is a close approximation to the linear portion of the desired calibration curve. This method has been used only in the case of relatively small drift and should be checked by a complete calibration after the set of observations.

PHOTOGRAPHIC PROCEDURE

The light source is an open air spark created by the discharge across a 1/8 inch gap of a 10 microfarad condenser charged to 7500 volts (design value) The light from the spark is reflected by a mirror so as to pass upward through the liquid in the glass-bottom ripple tank and then impinge upon the sensitized paper.

The sensitized paper used is 18 inch wide record paper (Grade B, Substance 28) as prepared by the Haloid Company. The spark photograms made were approximately 18 by 24 inches. The distance from light source to sensitized paper was about nine feet. The photograms were developed in Eastman D72 Developer (diluted 8 to 1) for one minute.

A sheet of aluminum, stiffened so as to be reasonably plane and suspended over the ripple tank, served to support the sensitized paper during exposure. The paper was held flat against the aluminum sheet by means of the adhesive action of Eastman's Kodaflat Clear Solution.

MECHANICAL TIMER

The timer consists of a synchronous 110 volt 1800 rpm motor and a directly coupled lead screw having a pitch of 20 threads per inch (Fig. 11). A special nut rides the screw; the nut is prevented from turning by a bearing constrained by two guide rails on the base of the timer. Three microswitches are attached to the two guide rails and are tripped by projections on the driven nut. The switches can be moved along the rails; a scale allows time intervals between zero and four seconds to be set in advance. The driven member can be returned to its starting point by reversing the direction of rotation of the motor. Limit switches at each end of the lead screw cut the current to the motor when actuated by the driven nut.

The action of the electrically operated apparatus can be coordinated by means of the three microswitches. For example: the first switch activates the solenoids on the wave generators to trip the valves and initiate the waves, and also turns on the recording mechanism of the oscillograph; the second switch initiates the spark for making a photogram of the instantaneous wave configuration; the third switch turns off the recording mechanism of the oscillograph.

IV   ANALYSIS OF RESULTS

A preliminary experimental study was made of wave forms and of the effect of adding detergents to the working fluid. A number of hydraulic-jump interactions were investigated. The results are presented and discussed.

MEASUREMENTS

In the investigation of hydraulic-jump interactions two types of measurement are necessary: the measurement of the angles between waves from the photograms, and the measurement of liquid depths from the oscillograms.

The measurement of the angular relation of the waves from the photograms was accomplished by means of a drafting machine. The error introduced in measurement is approximately one-half degree. Errors difficult to express quantitatively are introduced by roughness of the wave-fronts of strong hydraulic jumps and by curvature of the reflected waves; however, these errors are believed not to exceed one or two degrees.

Determination of liquid depth consists in measuring the corresponding distance on the oscillogram and correcting this value to the actual depth by means of a calibration curve. The error in liquid depth introduced by this process is approximately four per cent or less for the depths encountered.

Two less tangible factors tend to introduce error into the

measurement of liquid depth and thus influence reproduction of a wave of given strength. The first factor is the lack of smoothness behind strong and very weak hydraulic jumps or shock waves. The strong hydraulic jumps leave a rough and turbulent wake (Fig. 12a), while the very weak jumps are accompanied by secondary waves which create an oscillatory surface behind the shock front (Fig. 12b). This factor necessitates averaging the wave form by means of a somewhat arbitrary smooth curve before measurements can be made.

The second factor is a decay in strength as the shock progresses. This effect is more pronounced when a large diameter air inlet is employed on the generator; i.e., when the generator discharges rapidly. Under this condition, the capacity of the generator reservoir is not sufficient to keep the water depth constant behind the wave front until the wave has passed beyond the last measuring point. Thus an instantaneous section through the hydraulic jump shows an after-wave surface which slopes downward toward the rear. This lack of continual reinforcement results in a decrease in the strength of the shock as it progresses. The decay of wave strength is not so pronounced for the waves created under conditions which assure a continual discharge of water from the generator until the wave has passed the last measuring point. This condition (Fig. 12c) is obtained by using a large generator head and small diameter generator air inlets. In reproducing, or comparing waves with a marked decay in strength, it is important to make corresponding measurements at the same distance from the generator.

The velocities of a number of hydraulic jumps were calculated

from the oscillograph records and compared with the theoretical value given by Equation (20). The experimental value of velocity was in all cases higher than the theoretical value. A difference of as much as five per cent was found in the case of some strong waves. It has been suggested that this discrepancy is caused by a jet effect near the generator due to the fact that the velocity of the water as it leaves the generator is normally greater than the velocity of the wave generated. Also to be considered is the effect of wave strength decay. The velocity computed from the oscillogram is necessarily an average value, and, since the wave strength is decreasing throughout the measured distance, the problem arises of selecting the proper wave strength to use in the calculation of the theoretical velocity. For the weaker hydraulic jumps where the decay in strength is not so pronounced, the discrepancy between experimental and theoretical values of velocity is less than two per cent. Because of the above factors, measurements to determine wave strength and velocity should not be made too near the generator; a distance greater than 20 inches is desirable.

EFFECT OF ADDING DETERGENTS TO THE WORKING FLUID

The hydraulic jumps generated in the basic working fluid of distilled water had rough surfaces and the slopes of the wave-fronts were not so steep as desired (Fig. 13a).

In an attempt to improve wave shape and decrease roughness, 0.5 per cent by volume of "Isothan Q-15" (20% concentration of lauryl iso-quinolinium bromide) as prepared by the Onyx Oil and Chemical Company

was added to the working fluid. Hydraulic jumps created in the resulting fluid had the desired smoothness and a substantially increased wave-front slope (Fig. 13b); however, two disadvantages were apparent. First, suds were formed by each generated wave, and the resulting bubbles would interfere with photographic procedures. Second, the secondary waves accompanying the weaker shocks were also intensified, these secondary waves becoming evident with stronger shock waves than had been the case with no detergent. The range of strengths giving desirable wave forms thus shifted to higher values, an unsatisfactory situation in view of the fact that future plans were to investigate as weak hydraulic jumps as possible.

To obtain an intermediate effect, 0.5 per cent by volume of Kodak Photo-Flo (an aerosol solution) was added to the distilled water. Hydraulic jumps created in this fluid had the desired smoothness and a substantial increase in wave-front slope when compared with corresponding waves generated in distilled water (Fig. 13c). The advantage lay in the absence of bubbles to interfere with photographic procedures, and in the obtaining of weaker waves with more satisfactory form than were possible in the Isothan Q-15 solution.

The use of these detergents had no measurable effect on either the velocity or the strength of the hydraulic jumps, other variables remaining constant.

INTERACTION OF HYDRAULIC JUMPS

This investigation was concerned principally with the Mach

interactions of hydraulic jumps. Four sets of observations were
made with the primary purpose of determining experimentally the
strength and angular relation of the reflected wave. Test parameters
and results of the observations are presented in Tables I through IV.

The intermediate strength $\xi = 0.45$ was chosen as the weakest
for which a satisfactory wave-form could be obtained using an aerosol
solution as working fluid. The strong shock waves of strength $\xi = 0.28$ utilized the same test parameters except generator air inlet
diameter; therefore, the observations of strong and intermediate
strength waves could be made concurrently. The weak waves ($\xi = 0.70$) were generated in distilled water ($MnCl_2$ added) since a more
satisfactory wave form was thus realized than in the aerosol solution.
The upper limit of experimental values was determined by the weakest
reflected wave which could be detected on the photograms.

In Figs. 14 through 17 the strength ξ' of the reflected wave
is plotted as ordinate vs. the incident angle α as abscissa. The
theoretical curves were obtained from Fig. 4.

For presentation of the angular relation of the reflected wave,
the parameter usually chosen is $\alpha - \alpha'$ (see Figs. 1 and 2), which
represents the difference between the angle of incidence and the angle
of reflection. The values of $\alpha - \alpha'$ are plotted as ordinate vs. the
incident angle α as abscissa in Figs. 18, 20, 21 and 22. The theo-
retical curves were obtained from Fig. 3.

If the shock wave angles are measured with respect to the

direction of motion of the triple point of the Mach intersection,
the results should be independent of any curvature of the waves.
The experimentally determined relation between the angle δ (see
Fig. 2) representing the direction of motion of the triple point and
the incident angle α is presented in Fig. 24. In Figs. 25, 27, 28
and 29 the modified angle of reflection $\omega' (= \alpha' + \delta)$ is plotted as
ordinate vs. the modified incident angle $\omega (= \alpha - \delta)$ as abscissa.
In these figures the theoretical curves for regular interactions
were obtained from Reference 8; for Mach interactions the theoretical
values were obtained from Reference 19.

COMPARISON OF EXPERIMENT WITH THEORY

In all cases studied there is a definite disagreement between
experimental and theoretical values for Mach interactions and some
disagreement is indicated for regular interactions.

Consider the relation between ξ' and α presented in Figs. 14
through 17. The lower limit of Mach intersections occurs at the pre-
dicted value for strong and medium hydraulic jumps, but at a higher
value for weak jumps. Theory predicts a discontinuity between the
curves for regular and Mach intersections: experiment shows a smooth
transition from one configuration to the other. Also, no upper limit
of values for Mach intersections was reached experimentally.

Similar discrepancies are noted in the relations between $\alpha - \alpha'$
and α (Figs. 18, 20, 21 and 22) except that the experimental values
reach a minimum in the neighborhood of the transition from regular to

Mach intersections. Enough data in this region are not available to determine or disprove the existence of a discontinuity.

The relations of Figs. 18 and 22 for the interaction of hydraulic jumps can be compared with the corresponding relations of Figs. 19 and 23 respectively for the reflection of compression shocks in air. Figs. 19 and 23 are from Gilmore[11] who used the experimental results of Harrison and Bleakney.[16] For strong shocks in air the Mach theory gives a reasonable approximation to experiment (Fig. 19). The theoretical curves for shock and hydraulic jump interactions are analogous; but, since it has been found that the physical analogy is inexact for strong shocks, the discrepancies of Fig. 18 might be expected. For weak shocks in air the Mach theory evidences considerable disagreement with experiment (Fig. 23) although the disagreement is in the opposite direction to that for hydraulic jumps (Fig. 22).

Measurement of the angle of incidence and angle of reflection with respect to the line of motion of the triple point in order to allow for curvature of the shock waves did not alleviate the discrepancies between experiment and theory (Figs. 25, 27, 28 and 29). The disagreement is very marked for Mach interactions: a slight disagreement is evident for regular intersections.

Harrison and Bleakney[16] have presented data for the relation between ω and ω' in the case of compression shocks in air: the data for strong and weak shocks are presented in Figs. 26 and 30. Figs. 25 and 26 show corresponding data for strong shock waves in water and

air respectively: no resemblance is noted in the discrepancies
between experiment and Mach theory in the two cases. The trends
of experimental data are seen to be more similar in the cases of
weak shock waves in water and air (Fig. 29 and 30). For air, the
experimental values terminate at the extreme sonic point, which
represents a configuration in which incident and Mach shocks are
aligned, and the reflected shock has a strength $\xi' = 1.0$. For water
this limiting configuration is indicated by the dashed curve: experi-
mental values are found which exceed this limit.

Because of the definite disagreement of experiment with theory
for the Mach interactions of hydraulic jumps, the oscillograms and
photograms pertaining to the interactions were studied for information
leading to the source of the disagreement.

An examination of the oscillograms produced an important factor:
the depth h_4 behind the Mach wave is not equal to the depth h_3
behind the reflected wave (see Fig. 2). Thus the assumption used in
the development of the Mach theory, that the discontinuity is one of
velocity only, is not valid for hydraulic jumps.

The oscillograms also showed that a constant depth does not
exist between incident and reflected waves for the interaction of
weak hydraulic jumps ($\xi = 0.70$). In the cases of medium and strong
hydraulic jumps, no deviation from constant depth between waves was
detectable. This finding should be modified by two factors: the
weak hydraulic jumps were generated in water with no detergent; and
at most only two depth-measuring electrodes covered the area between

the incident and reflected waves.

Photograms of typical hydraulic-jump interactions are reproduced in Figs. 31 through 36. Figure 31 shows the Mach intersection of two equal strong hydraulic jumps. The next three figures show the development of the Mach intersection of two equal hydraulic jumps of intermediate strength. The three photograms are not of the same wave but show three different waves alike within experimental error. The reflection of a wave similar to those in Fig. 32 is presented in Fig. 35, and the intersection of two equal weak hydraulic jumps is presented in Fig. 36.

The most noticeable feature of these interactions is the Mach wave. This wave is convex for strong and medium hydraulic jumps, but is concave for the weak jumps as in the case of interactions of shocks in air. In general the convex Mach waves are not curved through their full length but have a straight center portion with curved ends.

Consider Fig. 34: the detail of the interaction is clearer in the case of intermediate strength hydraulic jumps. In the neighborhood of the triple point there appears to be a bending or curving of all three waves. This small bending is not consistent with other parameters and is not necessarily the same for two interactions with the same incident strength ξ and incident angle α. The measurement of wave angles with respect to the curvature of the Mach does not give satisfactory results unless the bending of the other waves is also considered. If the wave angles are measured in the immediate

neighborhood of the triple point and are plotted in the manner of
Fig. 20, the points do not lie in any logical sequence but do fall
nearly on a straight line (Fig. 37).

In the interactions of strong and intermediate strength hydraulic
jumps, a second wave is seen to follow the reflected wave. There is
no secondary incident wave which appears strong enough to have pro-
duced this secondary reflected wave. However, this wave can easily
be explained by the fact that the oscillograms show the depth behind
the Mach to be greater than the depth behind the reflected wave. In
this case, the secondary reflected wave also exists for the inter-
action of weak hydraulic jumps but this wave is too weak to be de-
tected on the photograms.

V   CONCLUSIONS

1.   There is a definite disagreement between experiment and theory for Mach interactions of hydraulic jumps.

2.   The assumption that the depth behind the Mach is equal to the depth behind the reflected wave is not valid. A wave separates these two areas rather than a velocity discontinuity.

3.   It is indicated that constant state between waves does not hold in the case of weak hydraulic-jump intersections, whereas constant state between waves holds for the interaction of strong and intermediate strength hydraulic jumps. A similar condition may exist in the case of interactions of shocks in air, explaining in part the greater disagreement of theory and experiment for weaker shocks.

4.   The Mach wave is convex for the interaction of strong and intermediate strength hydraulic jumps, but is concave in the case of weak hydraulic-jump intersections. The latter configuration exists for all shock reflections in air.

5.   For the Mach interactions of strong and intermediate strength hydraulic jumps, there is a curving of all three waves (Mach, incident and reflected) in the neighborhood of the triple point. Measurements should not be made so as to allow for curvature of the Mach without considering the curvature of the incident and reflected waves.

6.   The addition of a detergent to the working fluid results

in smoother waves and steeper shock fronts for hydraulic jumps of intermediate strength, but causes accentuation of the oscillatory nature of weaker hydraulic jumps.

7. It is recommended: (i) The theory of the Mach interactions of hydraulic jumps should be revised, taking into account the inequality of the depth behind the Mach and the depth behind the reflected wave. (ii) The lack of constant state between waves for the interaction of weak hydraulic jumps should be further investigated to determine the incident wave strength for which inconstancy of state first becomes experimentally detectable and to measure the amount of the deviation from constant state. (iii) Regular interactions of hydraulic jumps should be studied to determine whether the indicated disagreement between experiment and theory exists. (iv) The photographic procedure might be improved so that weaker reflected waves could be detected on the photograms. (v) The strength of incident wave for which the Mach changes from convex to concave should be determined. This transition point may bear some relation to the limit of reasonably exact analogy between shocks in air and surface shocks in liquids.

REFERENCES

1. Jouget, E., "Quelque Problèmes d'Hydrodynamique générale", J. de math. pures et appliq. (Series 8), 3, 1 (1920).

2. Riabouchinsky, D., "Sur l'analogie hydraulique des mouvements d'un fluide compressible", Compt. Rend. de l'acad. des sciences, 195, 998 (1932); 199, 632 (1934); 202, 1725 (1936).

3. Ippen, A., "An Analytical and Experimental Study of High Velocity Flow in Curved Sections of Open Channels", Thesis for PhD, Calif. Inst. of Technology, 1936.

4. Binnie, A. M., and Hooker, S. G., "The Flow under Gravity of an Incompressible and Inviscid Fluid through a Constriction in a Horizontal Channel", Proc. Roy. Soc., 159, 592 (1937).

5. von Kármán, Th., "Eine Praktische Anwendung der Analogie zwischen Überschall-Strömung in Gasen und überkritische Strömung in offenen Gerinnen", Z. für angew. Math. u. Mech., 18, 49 (1938).

6. Preiswerk, E., "Application of the Methods of Gas Dynamics to Water Flows with Free Surface; I. Flows with no Energy Dissipation; II. Flows with Momentum Discontinuities (Hydraulic Jumps)", NACA T.M. 934 and 935 (1940); translated from "Mitteilungen aus dem Institut für Aerodynamik", Nr. 7, Eidg. Tech. Hochsch., Zurich (1938).

7. Polacheck, H., and Seeger, R. J., "Regular Reflection of Shocks

in Ideal Gases", Explosives Research Report No. 13, Navy Dept., BuOrd, Washington, D. C., Feb. 1944.

8. Polacheck, H., and Seeger, R. J., "Interaction of Shock-Waves in Water-like Substances", Explosives Research Report No. 14, Navy Dept., BuOrd, Washington, D.C., Aug. 1944.

9. Stoker, J. J., "The Formation of Breakers and Bores", Commun. on Applied Math., 1, 1 (1948).

10. Friedrichs, K. O., "On the Derivation of the Shallow Water Theory" (appendix to Ref. 9), Commun. on Applied Math., 1, 81 (1948).

11. Gilmore, F. R., "The Analogy between the Flow of a Liquid with a Free Surface and the Two-Dimensional Flow of a Gas", Memorandum Report No. M-54.1, Hydrodynamics Laboratory, Calif. Inst. of Technology, March 1949.

12. Bruman, J. R., "Application of the Water Channel - Compressible Gas Analogy", Report NA-47-87, North American Aviation, Inglewood, Calif., March 3, 1947.

13. Johnson, R. H., Nial, W., and Witbeck, N., "Water Analogy to Two-Dimensional Air Flow", Report No. 55218, General Electric Co., Schenectady, N. Y., August 28, 1947.

14. von Neumann, J., "Oblique Reflection of Shocks", Explosives Research Report No. 12, Navy Dept., BuOrd, Washington, D. C., Oct. 1943.

15. Keenan, P. C., and Seeger, R. J., "Analysis of Data on Shock Intersections Progress Report 1", <u>Explosives Research Report No. 15</u>, Navy Dept., BuOrd, Washington, D. C., Feb. 1944.

16. Harrison, F. B., and Bleakney, W., "Remeasurement of Reflection Angles in Regular and Mach Reflection of Shock Waves", Physics Dept., Princeton Univ., March 1947.

17. Einstein, H. A., and Baird, E. G., "Progress Report of the Analogy between Surface Shock Waves on Liquids and Shocks in Compressible Gases", Hydrodynamics Laboratory, Calif. Inst. of Technology, Sept. 15, 1946.

18. Einstein, H. A., and Baird, E. G., "Progress Report of the Analogy between Surface Shock Waves on Liquids and Shocks in Compressible Gases", Hydrodynamics Laboratory, Calif. Inst. of Technology, July 30, 1947. (unpublished)

19. Liepmann, H. W., and Puckett, A. E., <u>Introduction to Aerodynamics of a Compressible Fluid</u>, J. Wiley and Sons, New York, 1947.

20. "Computations on Hydraulic Analogy of Shock Wave Intersections", prepared specifically for the Navy Dept., BuOrd, under the Mathematical Tables Project of the Applied Mathematics Panel, NDRC.

21. Lamb, Horace, <u>Hydrodynamics</u>, Sixth Edition, Dover Publications, New York, 1945.

22. Courant, R., and Friedrichs, K. O., <u>Supersonic Flow and Shock Waves</u>, Interscience Publishers Inc., New York, 1948.

TABLE   I

$$\xi = 0.28 \pm 0.02$$

Intersection of Two Equal Hydraulic Jumps

Liquid: 0.5 per cent by vol. Kodak Photo-Flo (aerosol solution) in

distilled water (0.001 to 0.002 normal $MnCl_2$).

Initial liquid depth: 6.95 ± 0.03 millimeters

α	α'	ξ'	δ	ω	ω'
29.2	25.5	0.48		29.2	25.5
33.8	28.0	0.58		33.8	28.0
40.8	41.2	0.56	1.2	39.6	42.4
46.0	49.1	0.62	2.7	43.3	51.8
51.8	42.5	0.66	4.4	47.4	46.9
56.2	39.5	0.68	6.0	50.2	45.5
61.0	37.5	0.72	7.8	53.2	45.3
65.0	33.0	0.76	9.0	56.0	42.0
70.0	31.0	0.80	11.0	59.0	42.0
75.5	29.0	0.84	14.0	61.5	43.0

TABLE   II

$$\xi = 0.45 \pm 0.02$$

Intersection of Two Equal Hydraulic Jumps

Liquid: 0.5 per cent by vol. Kodak Photo-Flo (aerosol solution) in

distilled water (0.001 to 0.002 normal $MnCl_2$).

Initial liquid depth: 6.95 ± 0.03 millimeters

a	a'	ξ'	δ	ω	ω'
28.8	27.5	0.60		28.8	27.5
33.5	31.5	0.62		33.5	31.5
40.8	44.0	0.68	0.4	40.4	44.4
46.0	48.0	0.70	1.8	44.2	49.8
51.5	47.0	0.71	3.4	48.1	50.4
56.5	46.0	0.73	4.9	51.6	50.9
62.0	42.0	0.76	6.6	55.4	48.6
66.0	36.0	0.82	8.0	58.0	44.0
71.2	34.0	0.86	9.9	61.4	43.9
75.8	31.5	0.92	11.9	63.9	43.4
79.8	27.2	- -	14.3	65.5	41.5

TABLE III

$$\xi = 0.45 \pm 0.02$$

Reflection of Hydraulic Jump from Rigid Wall

Liquid: 0.5 per cent by vol. Kodak Photo-Flo (aerosol solution) in distilled water (0.001 to 0.002 normal $MnCl_2$).

Initial liquid depth: 6.93 ± 0.03 millimeters

α	α'	ξ'	δ	ω	ω'
35.5	28.5	0.70		35.5	28.5
40.5	39.0	0.67	0.3	40.2	39.3
45.0	46.0	0.71	1.5	43.5	47.5
50.0	46.0	0.75	2.9	47.1	48.9
56.0	41.0	0.79	4.7	51.3	45.7
61.0	36.5	0.82	6.3	54.7	42.8
65.5	32.5	0.85	7.8	57.7	40.3
70.5	28.5	0.90	9.7	60.8	38.2

'

TABLE IV

$$\xi = 0.70 \pm 0.03$$

Intersection of Two Equal Hydraulic Jumps

Liquid: Distilled water (0.001 to 0.002 normal $MnCl_2$).

Initial liquid depth: 5.00 ± 0.03 millimeters

α	a'	ξ'	δ	ω	ω'
29.2	26.2	0.68		29.2	26.2
34.2	33.5	0.67		34.2	33.5
40.5	41.5	0.68		40.5	41.5
46.5	50.0	0.72		46.5	50.0
52.5	61.0	0.76		52.5	61.0
57.8	63.8	0.81	1.4	56.4	65.2
63.0	66.0	0.84	2.9	60.1	68.9
68.0	65.0	0.88	4.2	63.8	69.2
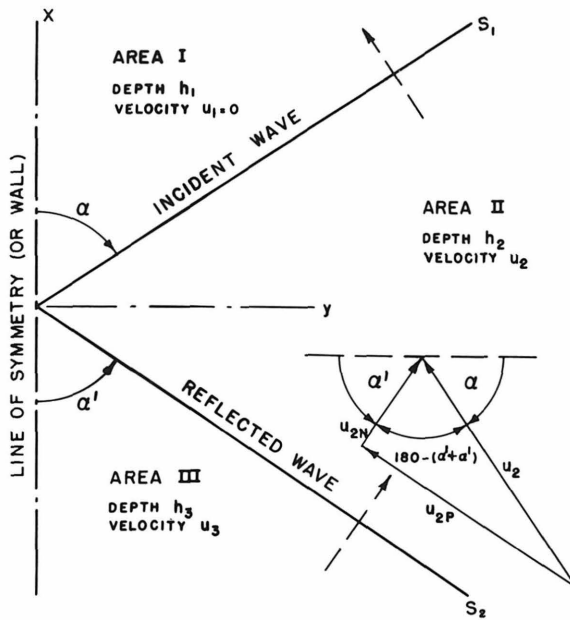
Fig. 1 Regular Intersection of Two Equal Hydraulic Jumps.
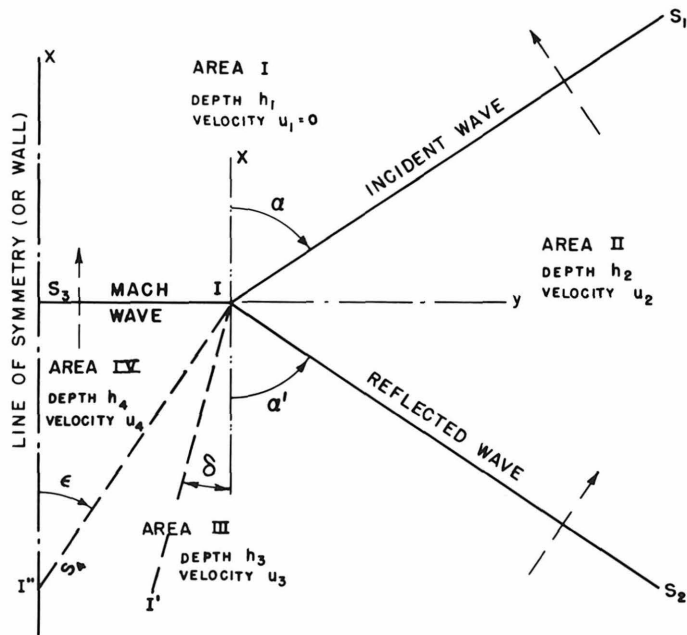
Fig. 2 Mach Intersection of Two Equal Hydraulic Jumps.
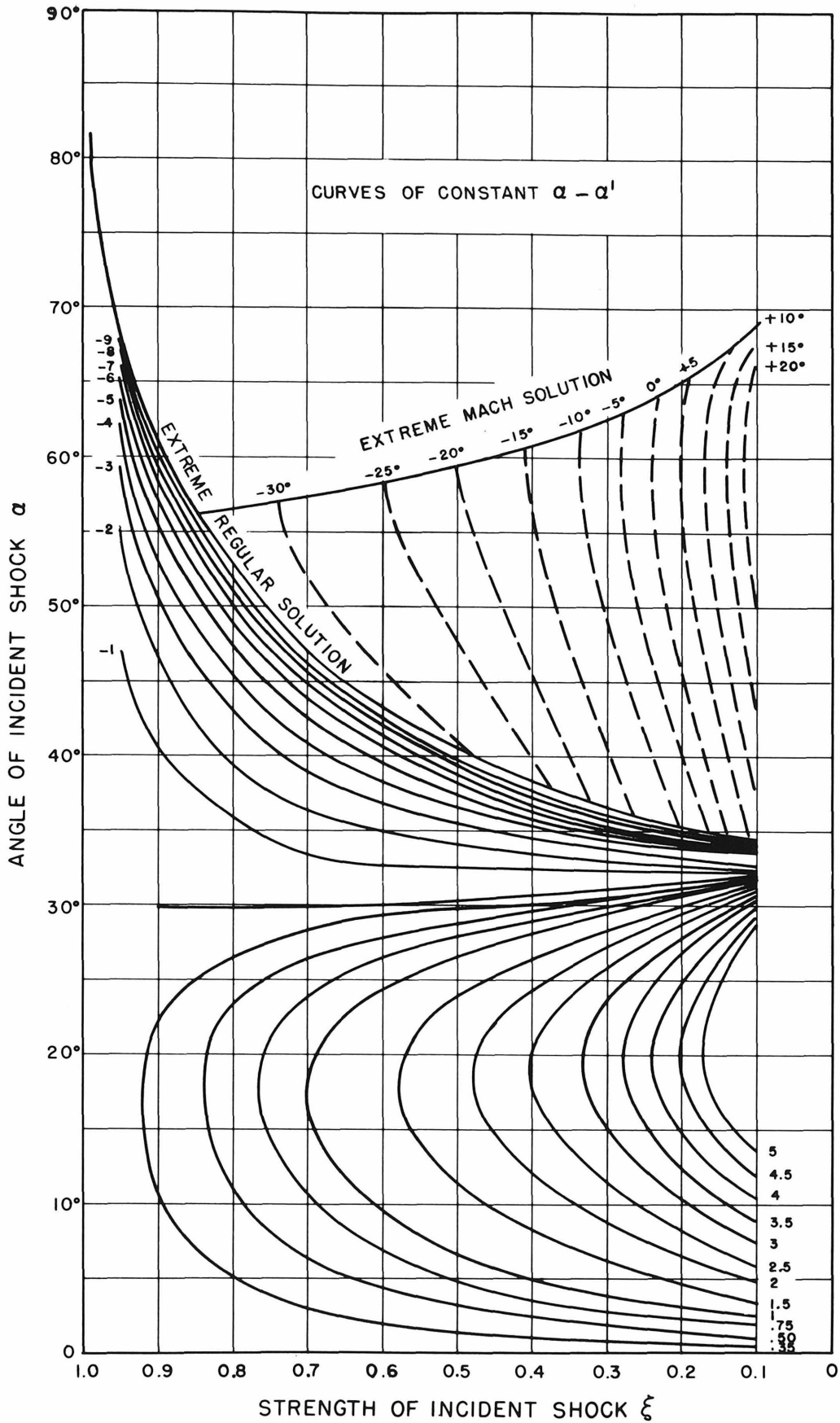
Fig. 3 Solutions for Shock-Wave Intersections Assuming Constant State between
Shocks, $\gamma = 2.00$ - Angle of Reflected Shock.
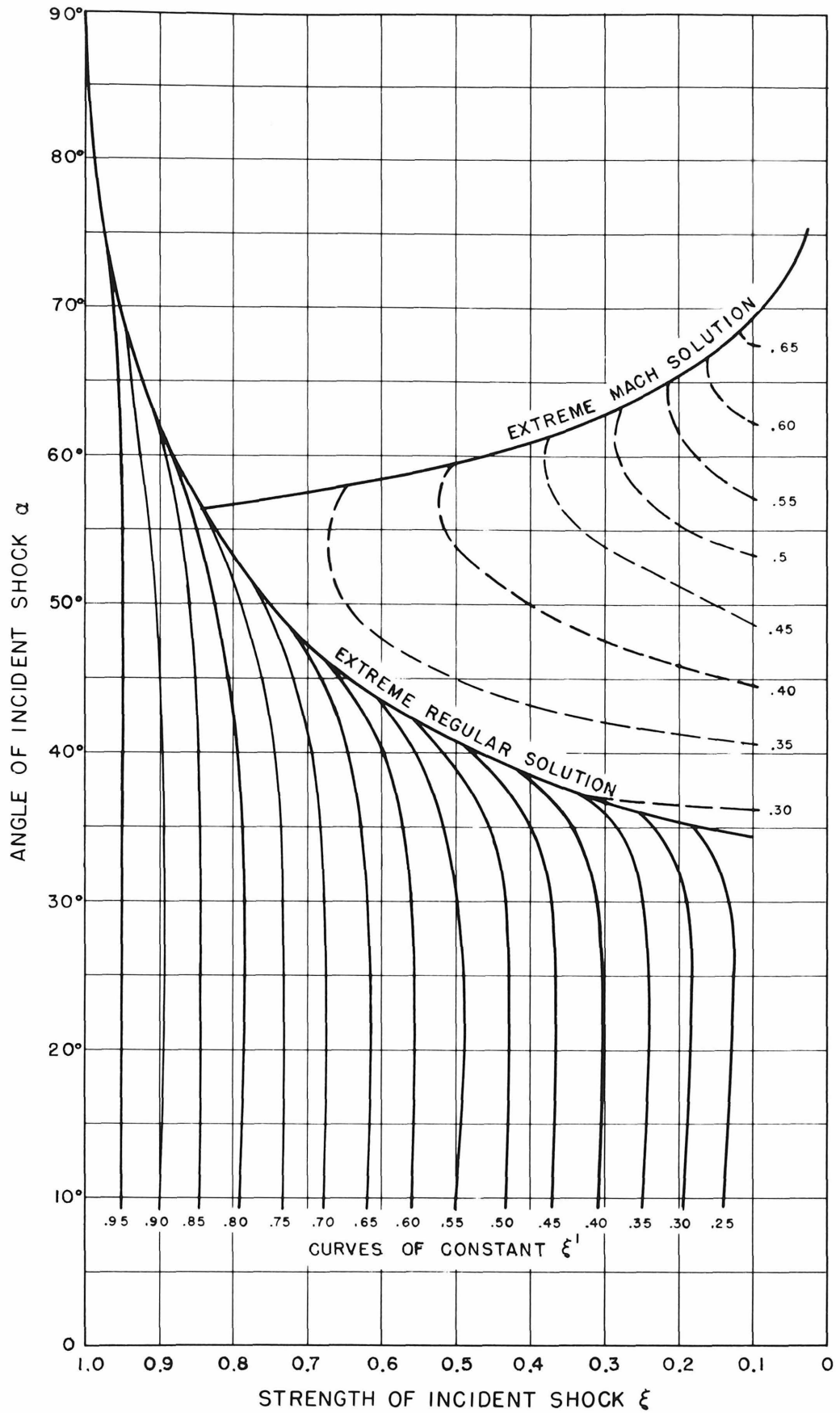
Fig. 4 Solutions for Shock-Wave Intersections Assuming Constant State between
Shocks, γ = 2.00 - Strength of Reflected Shock.
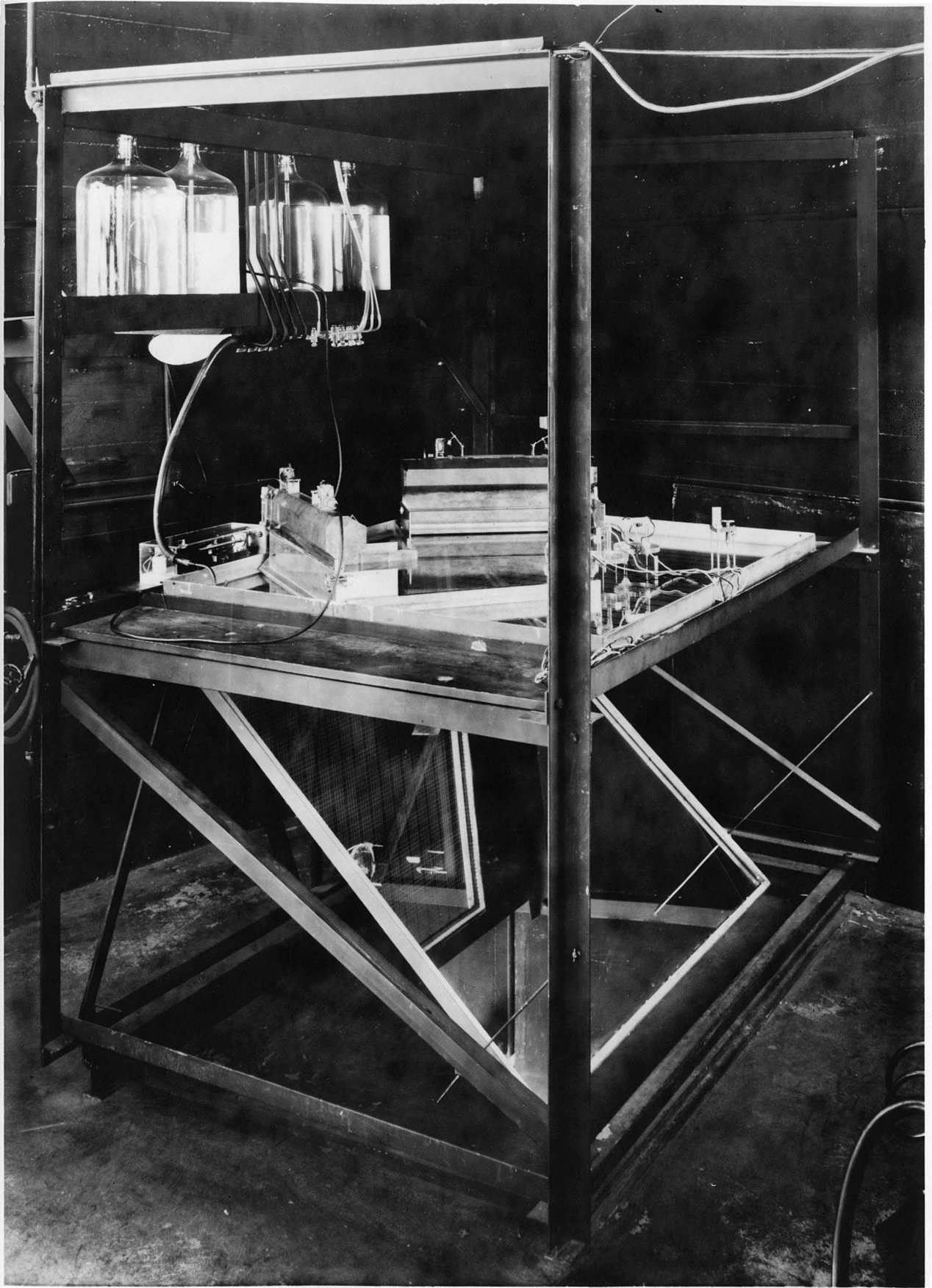
Fig. 5 The Ripple Tank.
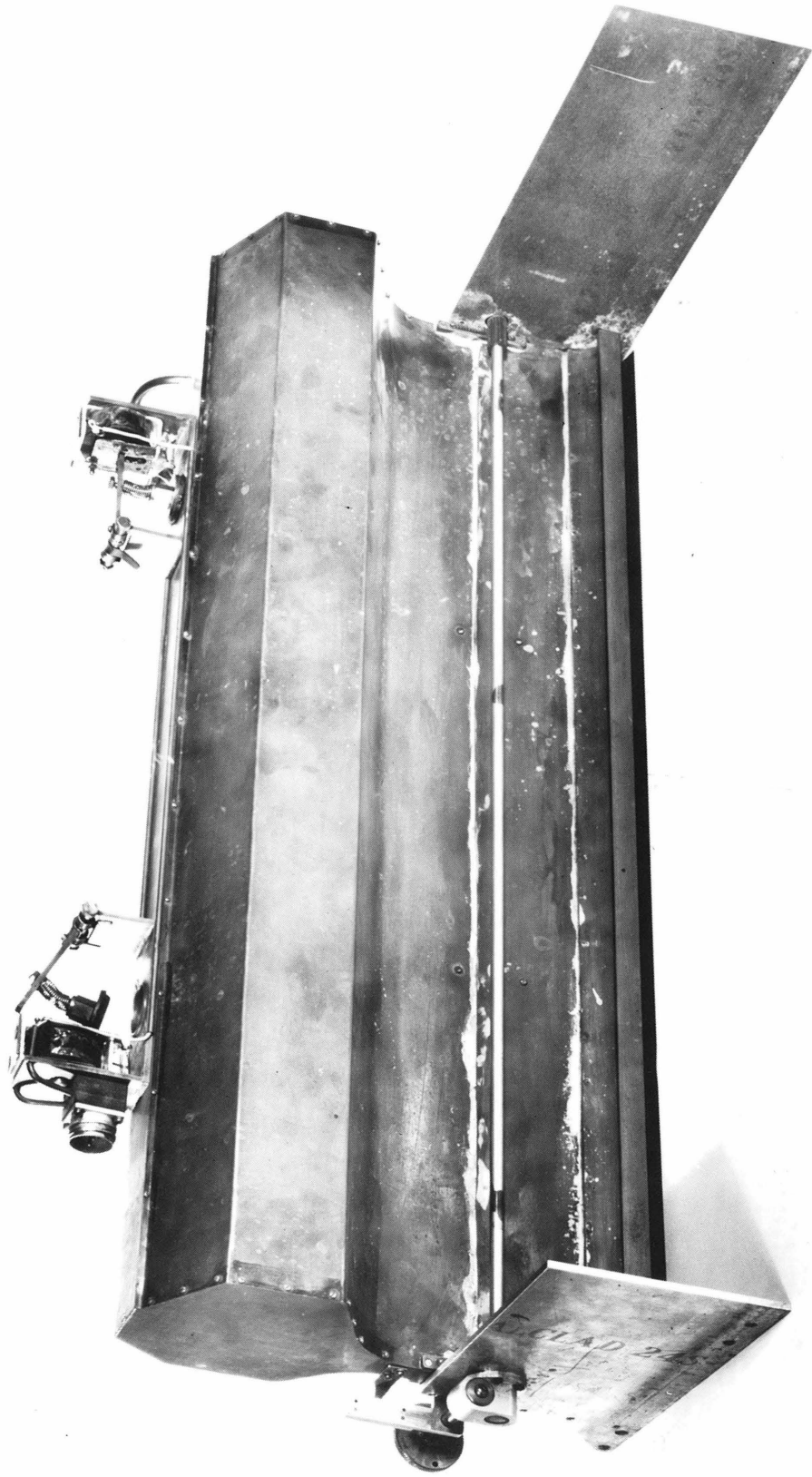
Fig. 6 The Wave Generator.
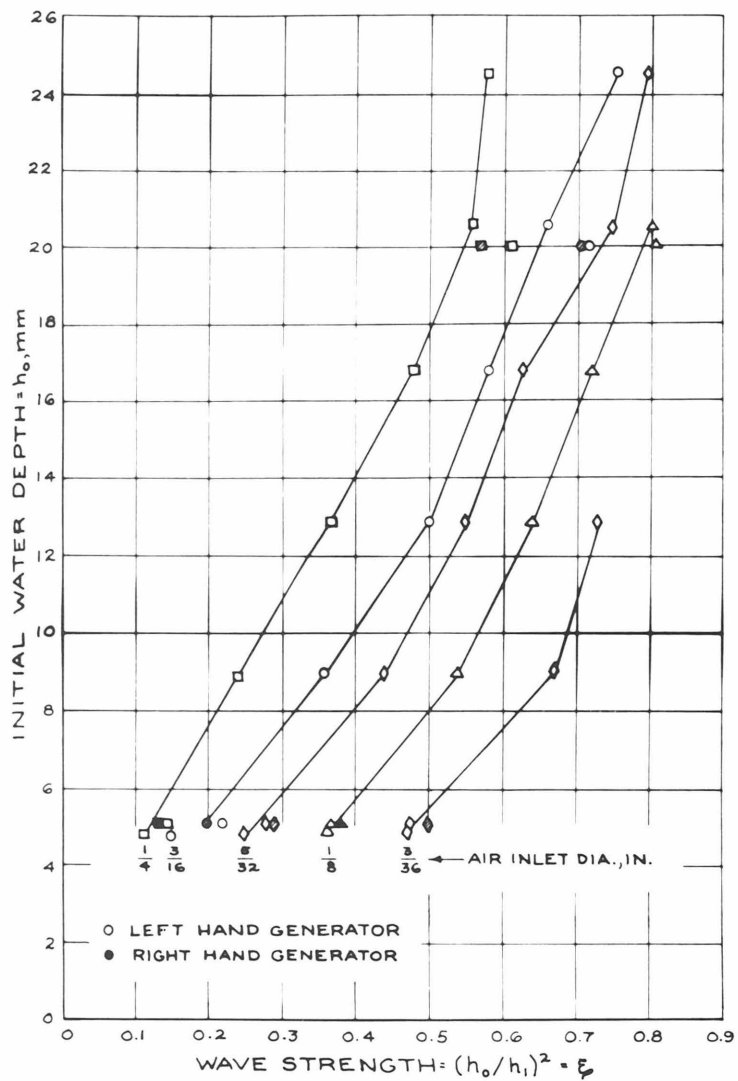
Fig. 7 Effect upon Wave Strength of Initial Water Depth and Diameter of Generator Air Inlet.
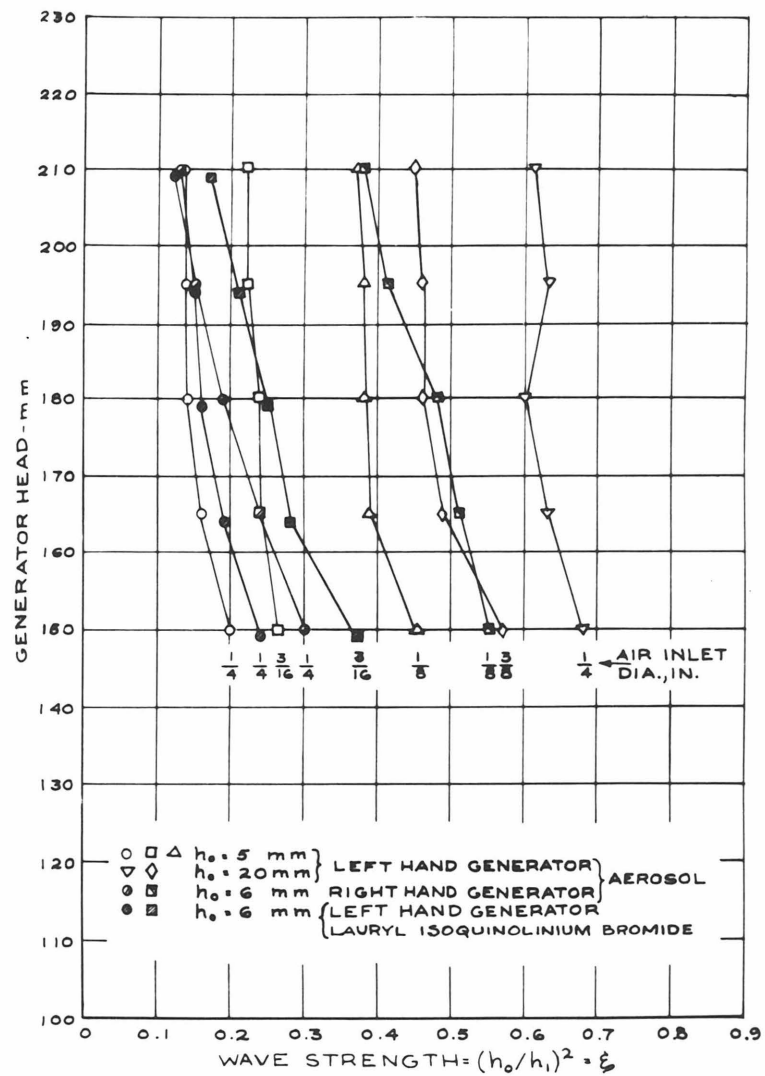
Fig. 8 Effect upon Wave Strength of Height to Which Water is Raised in the Generator.

REFLECTED WAVE

RIGHT HAND
PRIMARY WAVE

h_2

h_1

h_0

h_2

INTERSECTION

h_1

REFLECTED WAVE

LEFT HAND
PRIMARY WAVE

h_2

h_1

h_0
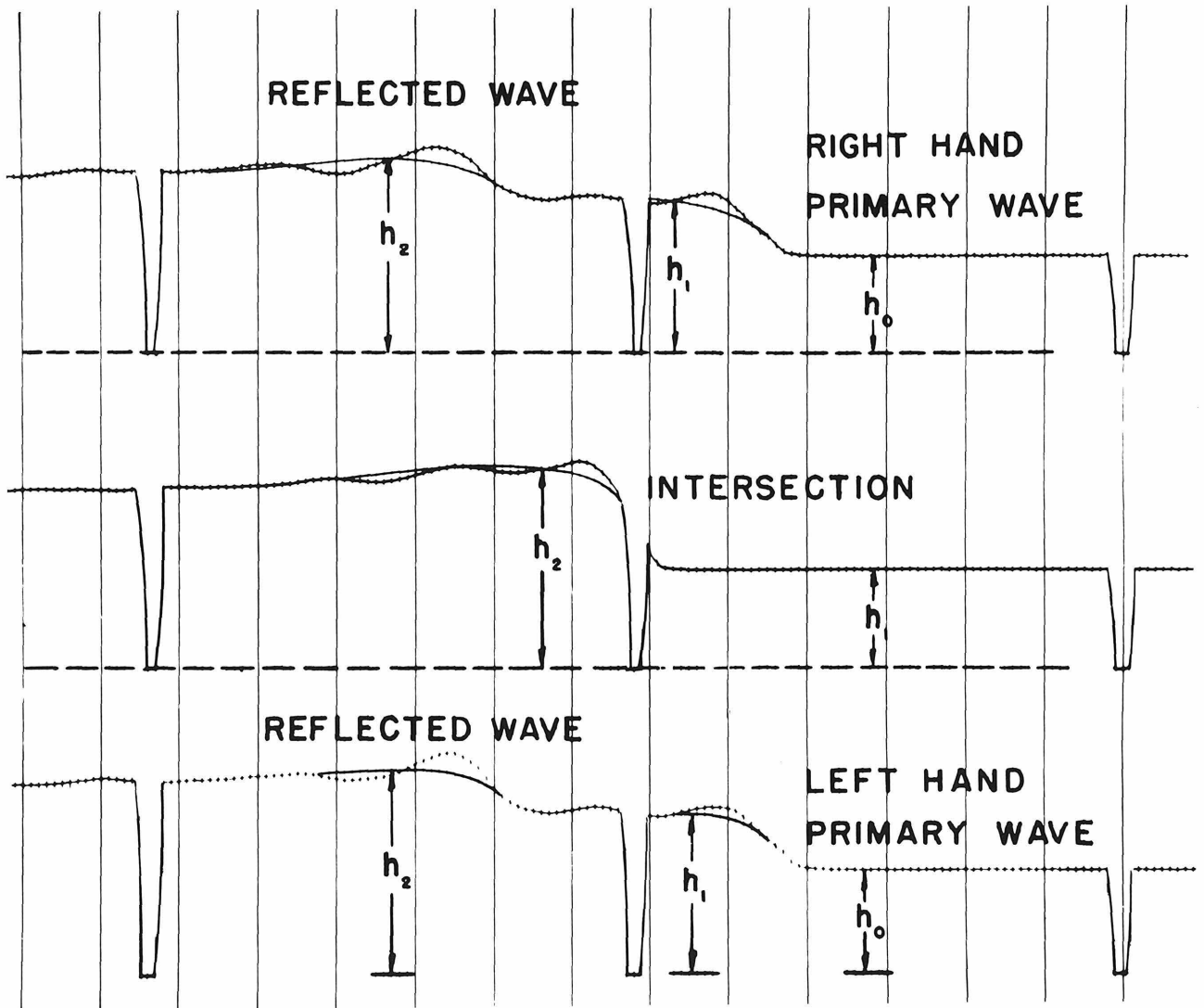
Fig. 9 Typical Oscillogram - Hydraulic-Jump Intersection.
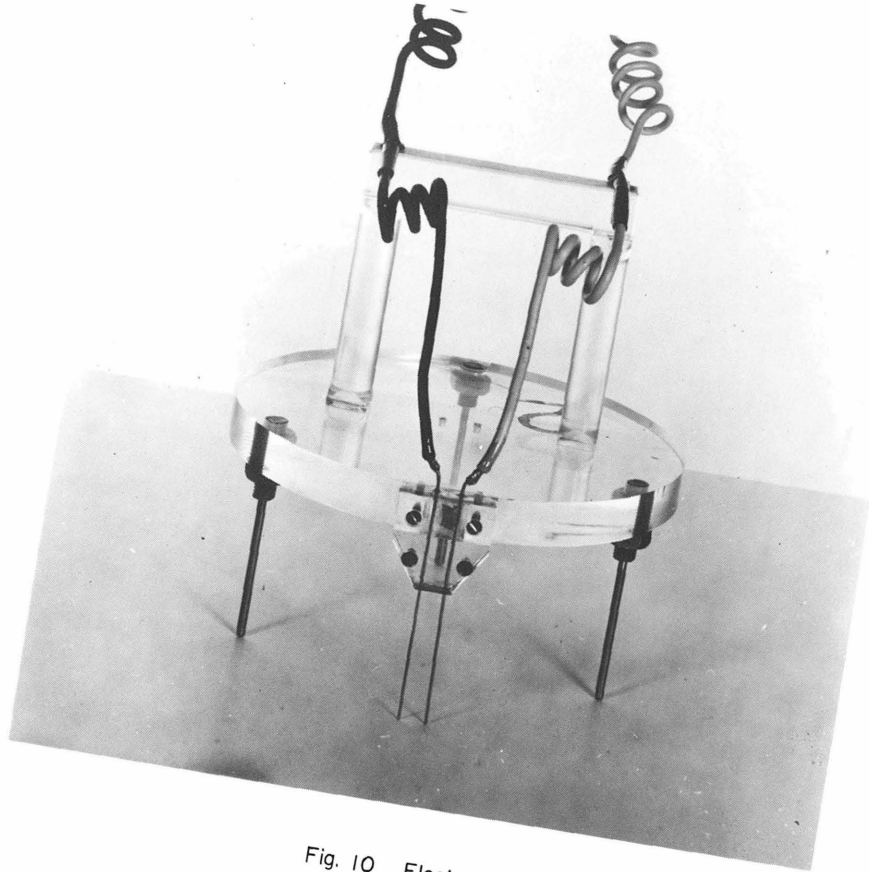
Fig. 10   Electrode.
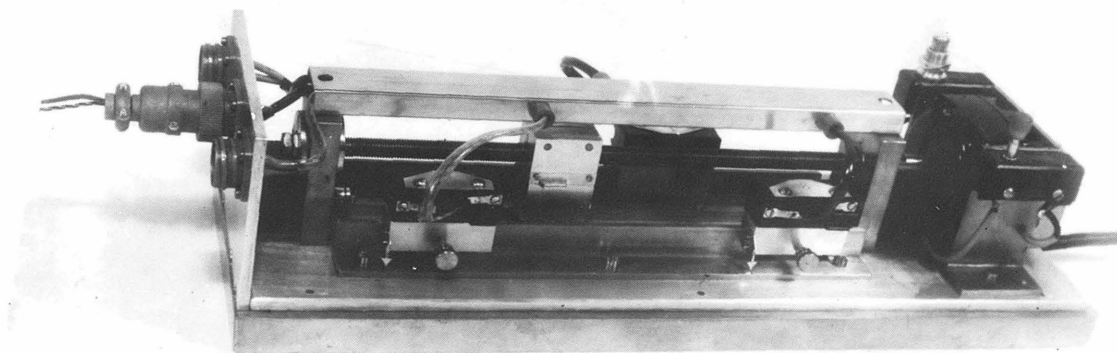
Fig. 11   The Mechanical Timer.

a. Strong Wave with Rough and Sloping After-Wave Surface.
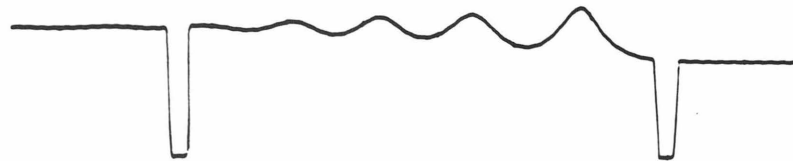
a. Distilled Water.

b. Weak Wave with Secondary Waves.

b. Lauryl Isoquinolinium Bromide Solution.

c. Satisfactory Wave Form.

c. Aerosol Solution.

Fig. 12 Typical Wave Forms.

Fig. 13 Comparison of Similar Waves Generated in Different Fluids.
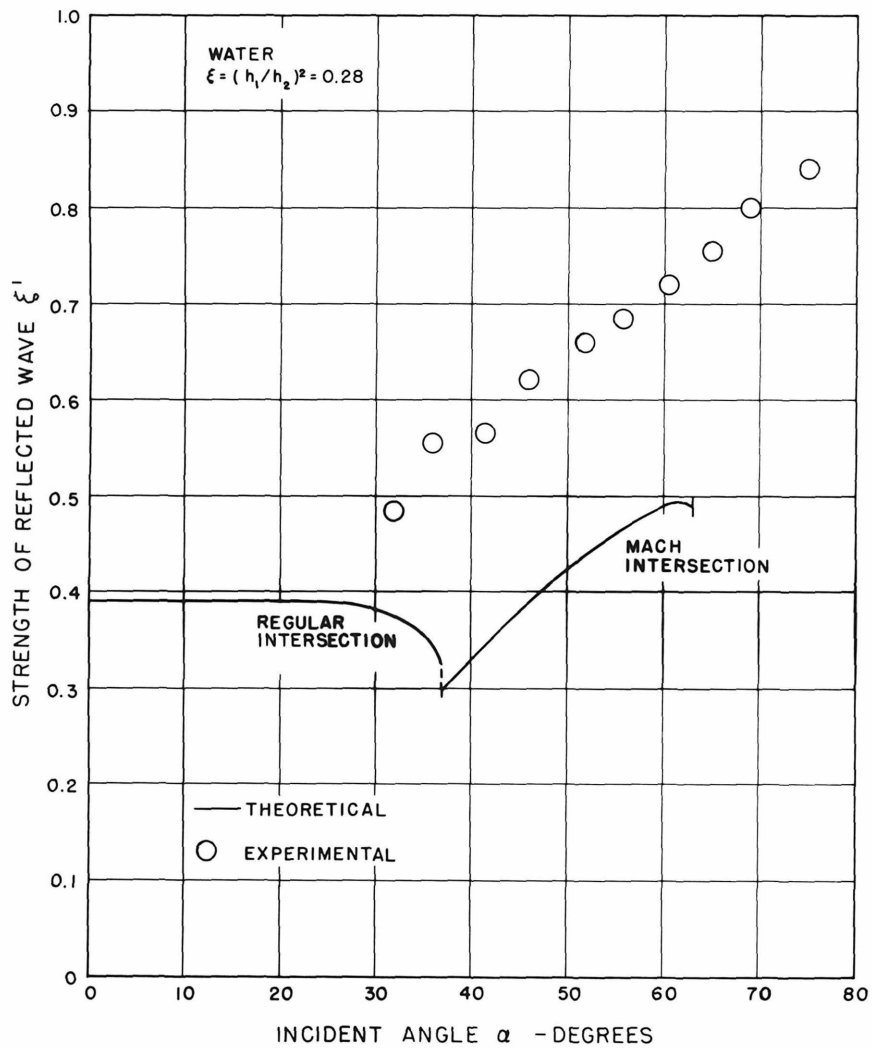
Fig. 14 Strength of Reflected Wave - Intersection of Two Equal Hydraulic Jumps of Strength $\xi = 0.28$.
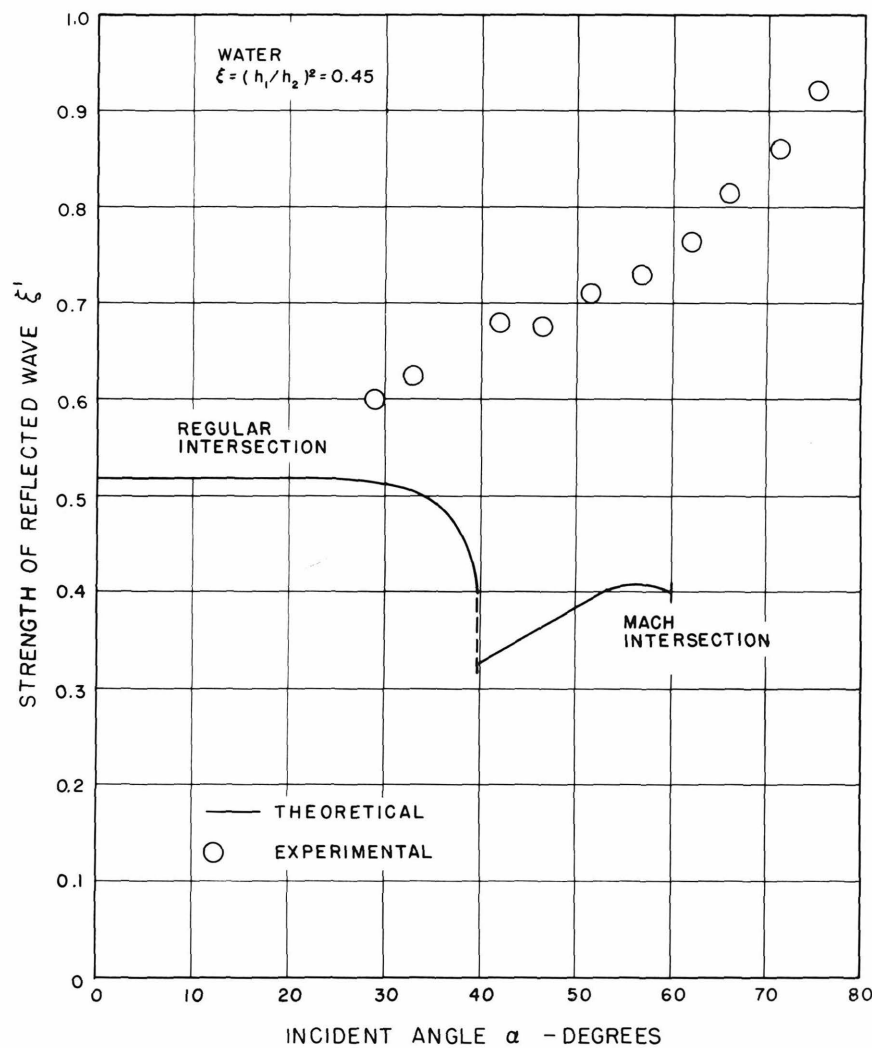
Fig. 15 Strength of Reflected Wave - Intersection of Two Equal Hydraulic Jumps of Strength $\xi = 0.45$.
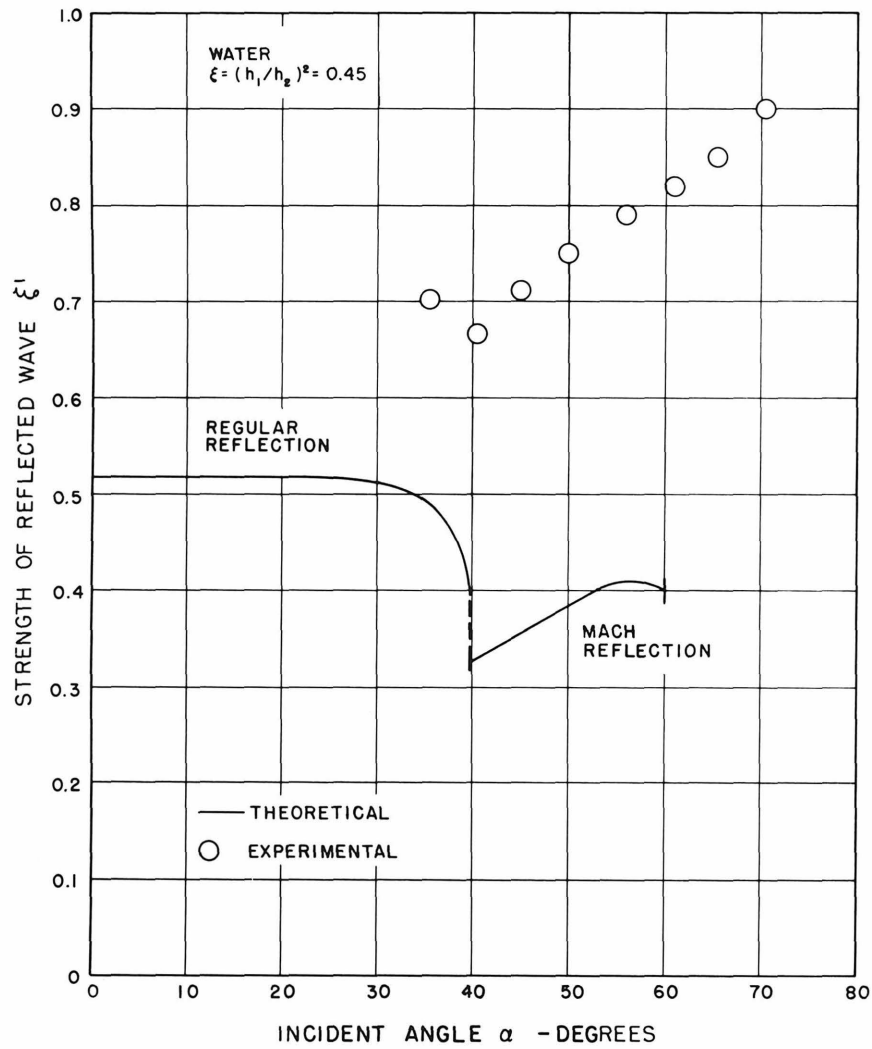
Fig. 16 Strength of Reflected Wave - Reflection from Rigid Wall of Hydraulic Jump of Strength ξ = 0.45.
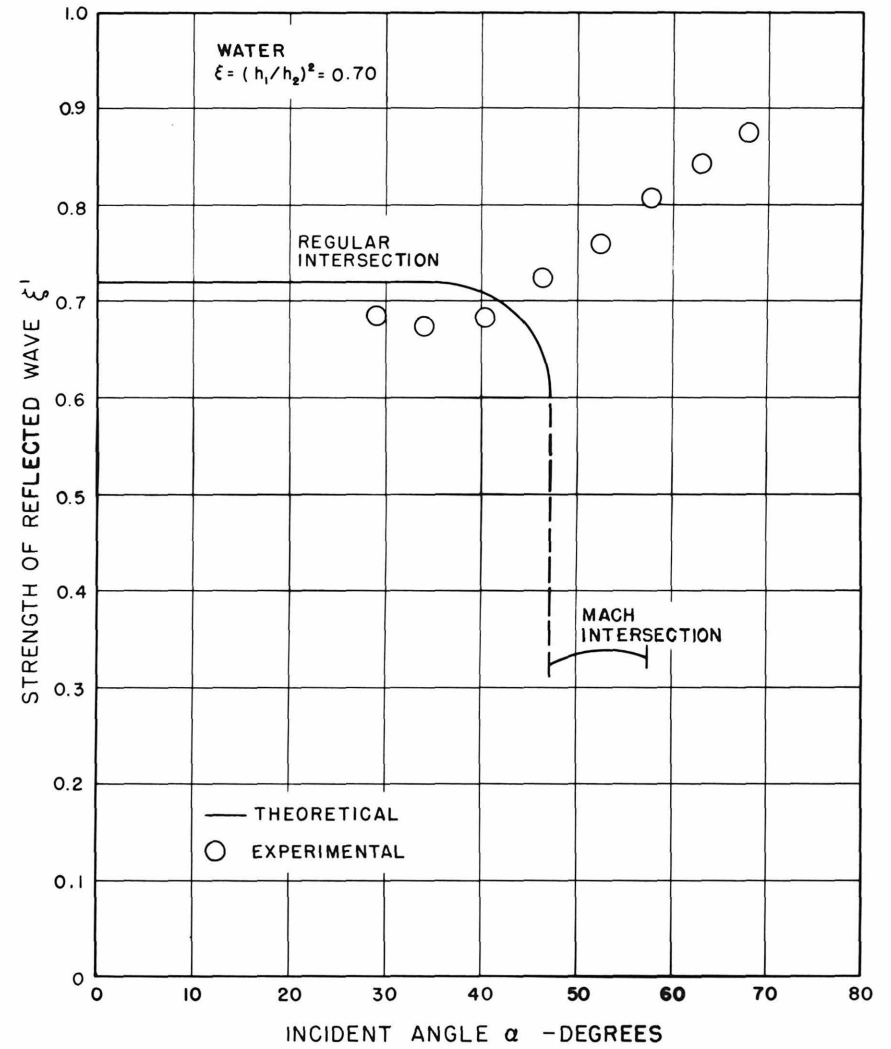
Fig. 17 Strength of Reflected Wave - Intersection of Two Equal Hydraulic Jumps of Strength ξ = 0.70.
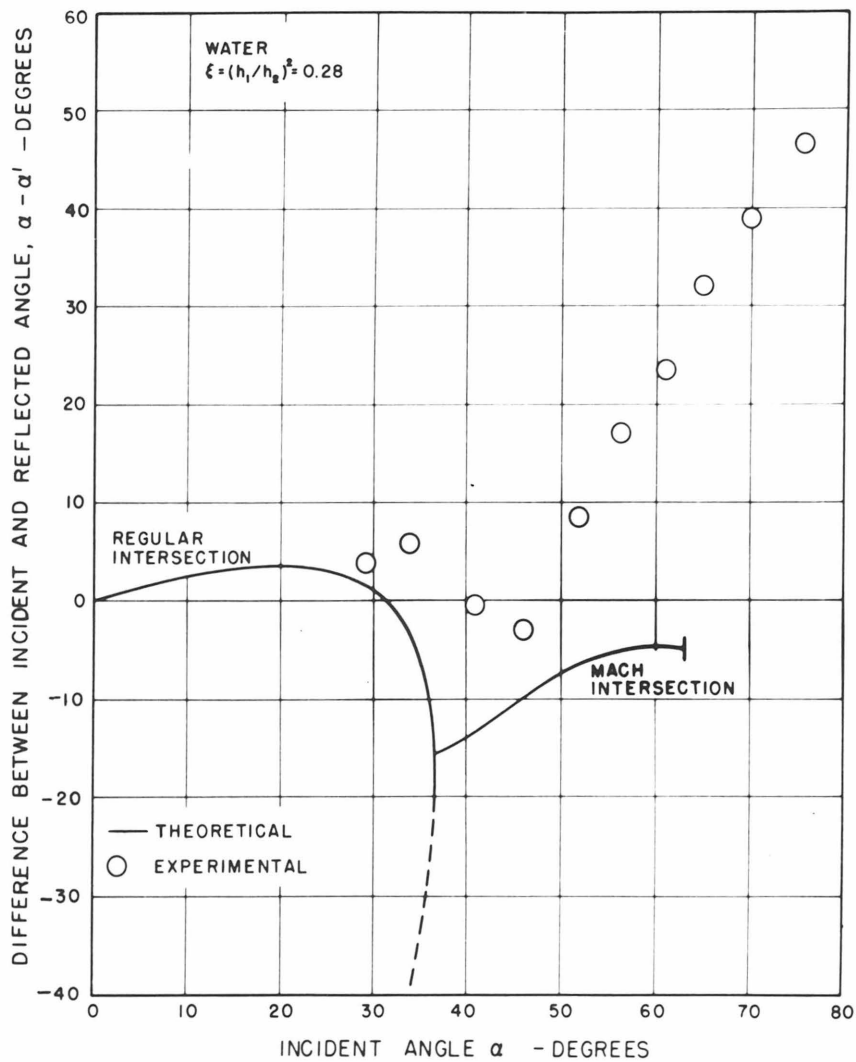
Fig. 18 Angle of Reflected Wave - Intersection of Two Equal Hydraulic Jumps of Strength ξ = 0.28.
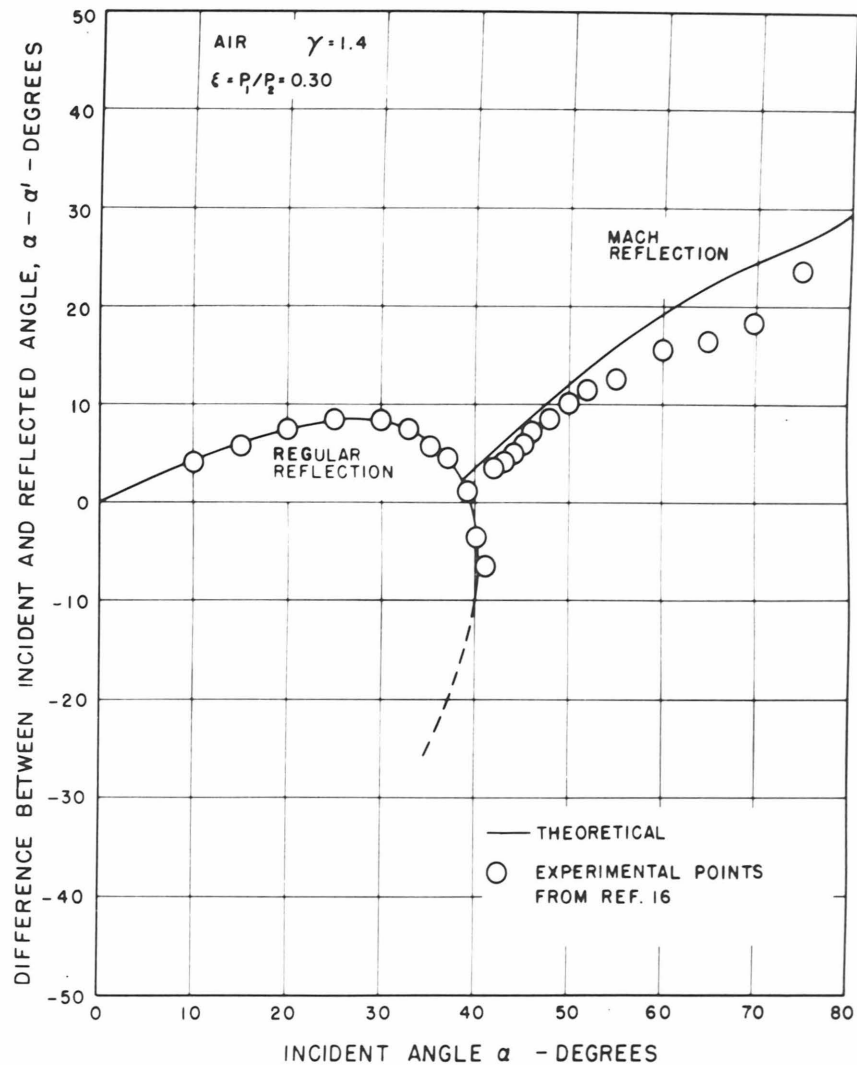
Fig. 19 Angle of Reflected Shock - Reflection of Compression Shock in Air, Pressure Ratio ξ = 0.30.

- 55 -
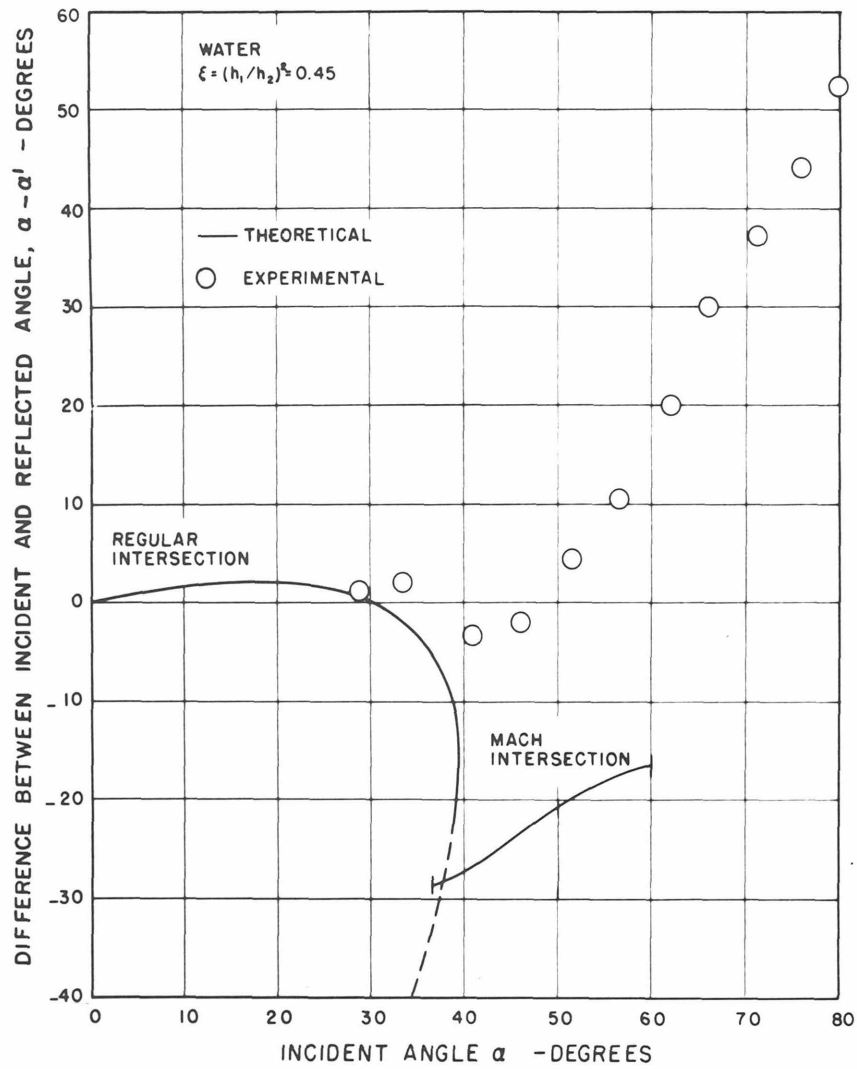
Fig. 20 Angle of Reflected Wave - Intersection of Two Equal Hydraulic Jumps of Strength ξ = 0.45.
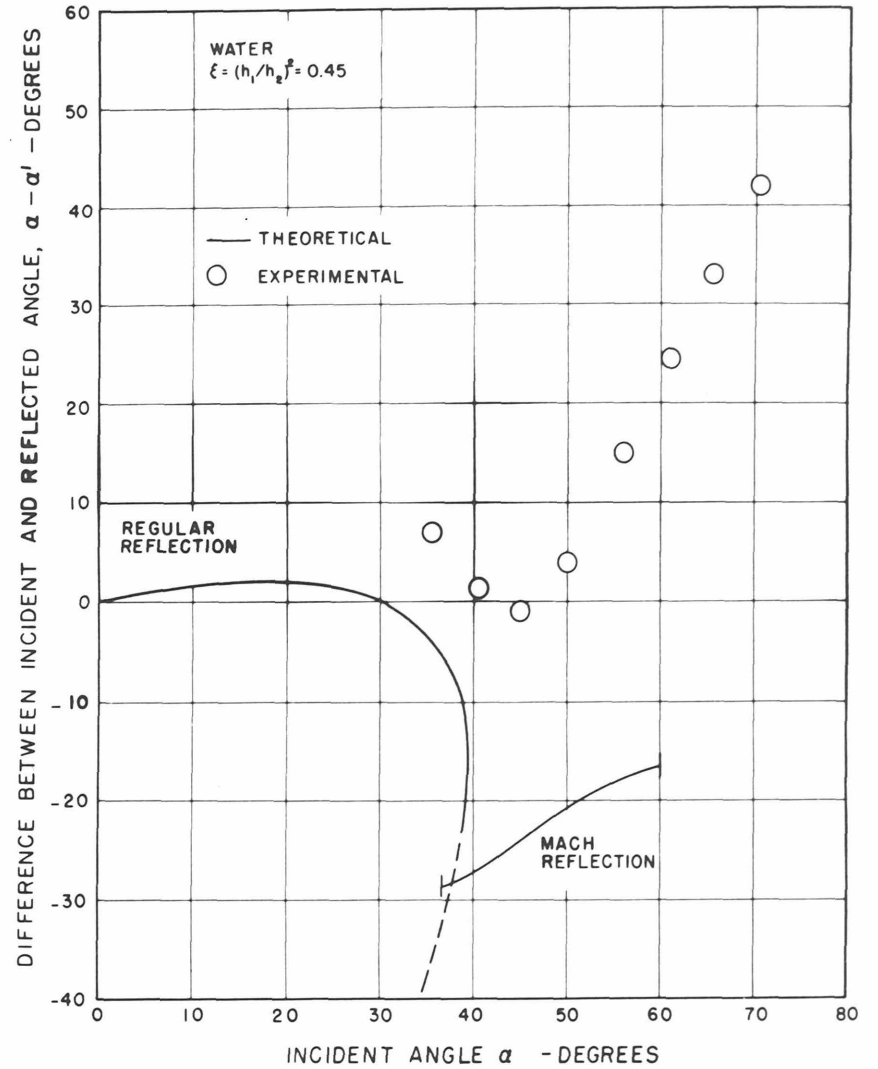
Fig 21 Angle of Reflected Wave - Reflection from Rigid Wall of Hydraulic Jump of Strength ξ = 0.45.
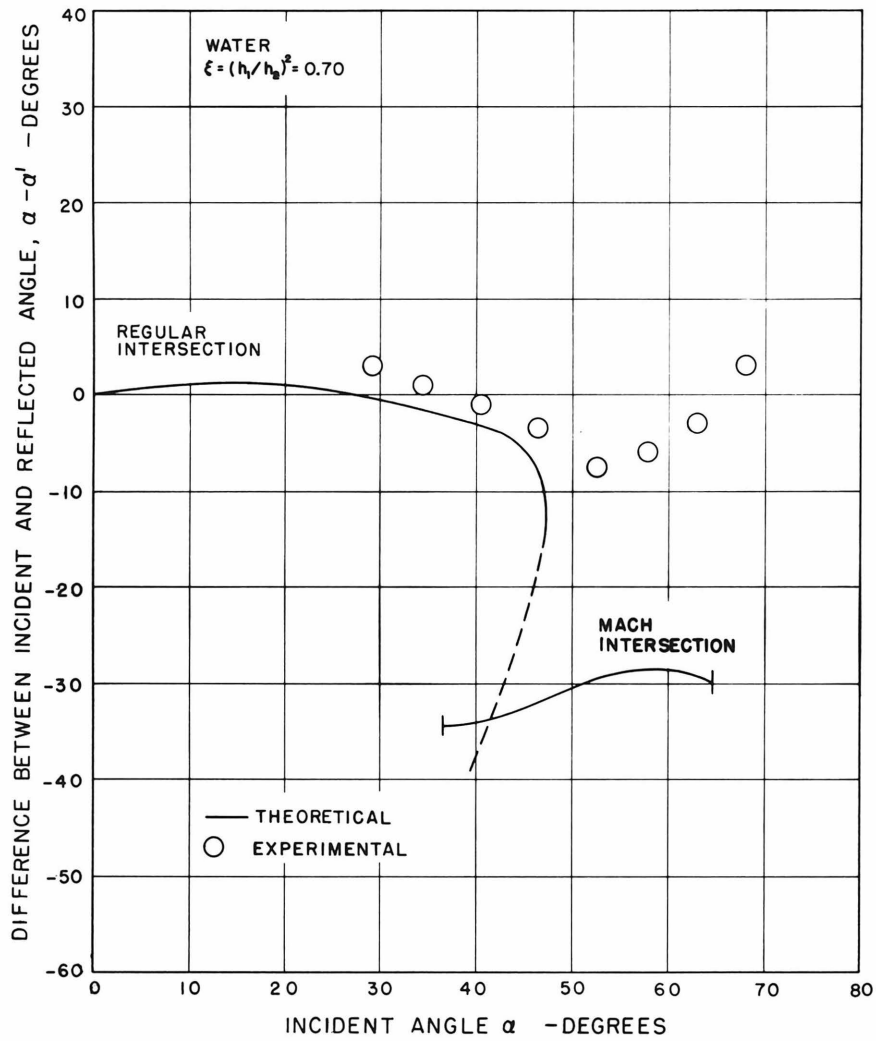
Fig. 22 Angle of Reflected Wave - Intersection of Two Equal Hydraulic Jumps of Strength $\xi = 0.70$.
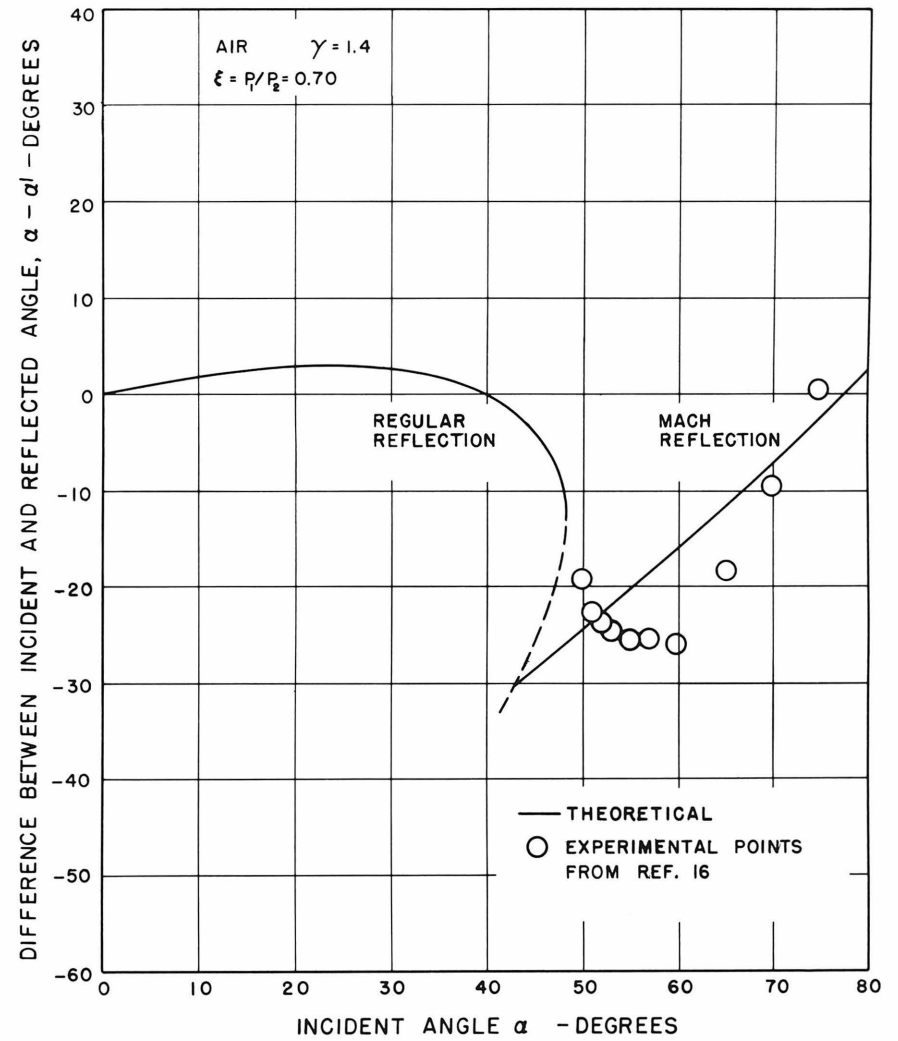
Fig. 23 Angle of Reflected Shock - Reflection of Compression Shock in Air, Pressure Ratio $\xi = 0.70$.
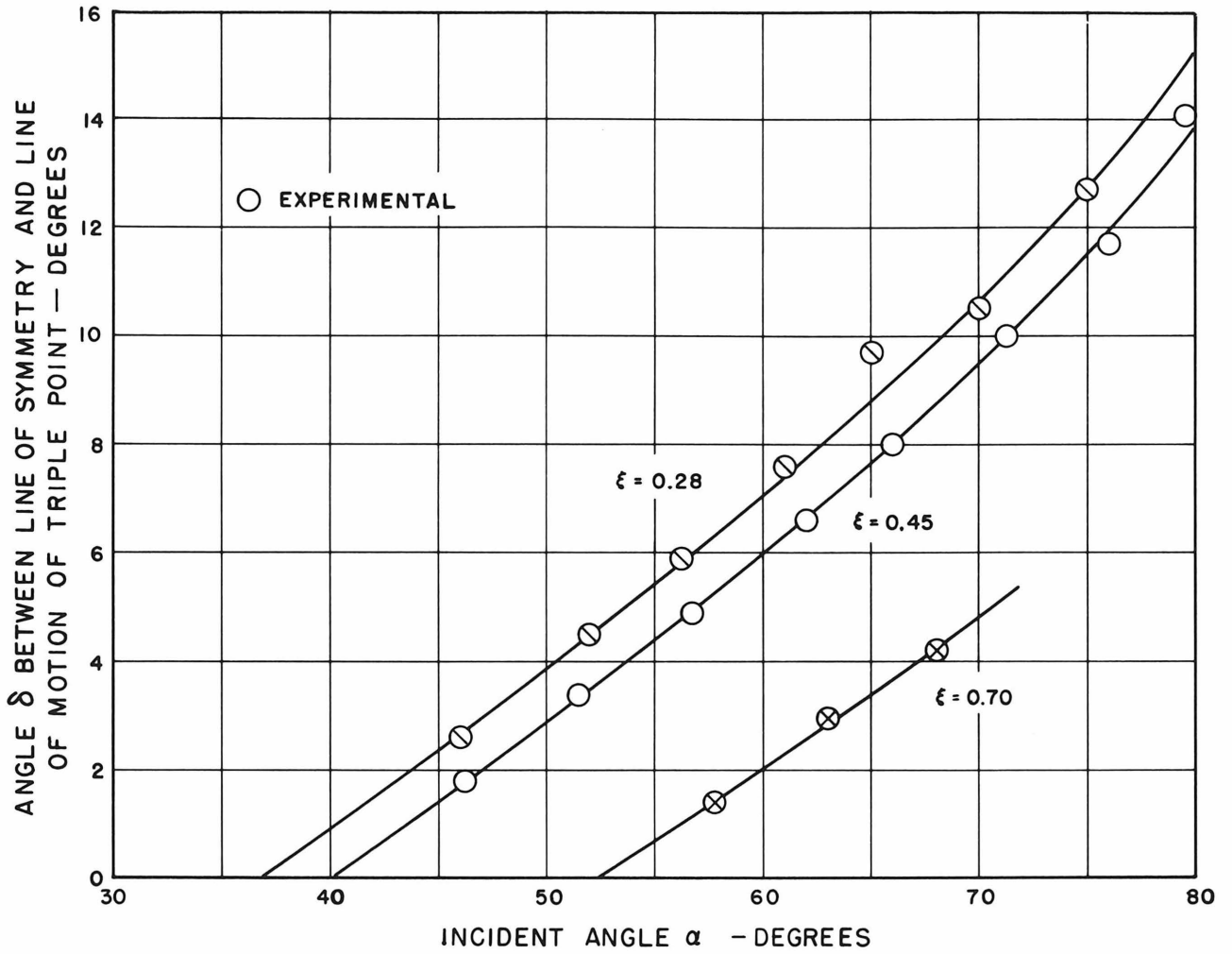
Fig. 24 Direction of Motion of Triple Point of Hydraulic-Jump Mach Intersections.
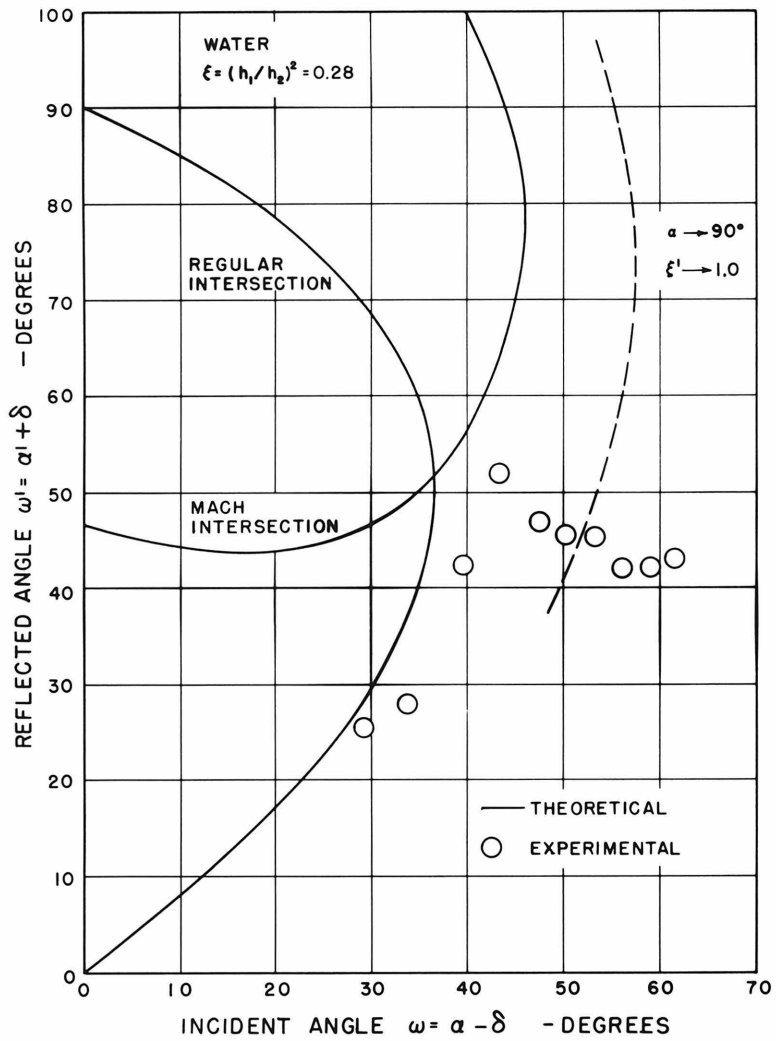
Fig. 25 Intersection of Two Equal Hydraulic Jumps of Strength $\xi = 0.28$.
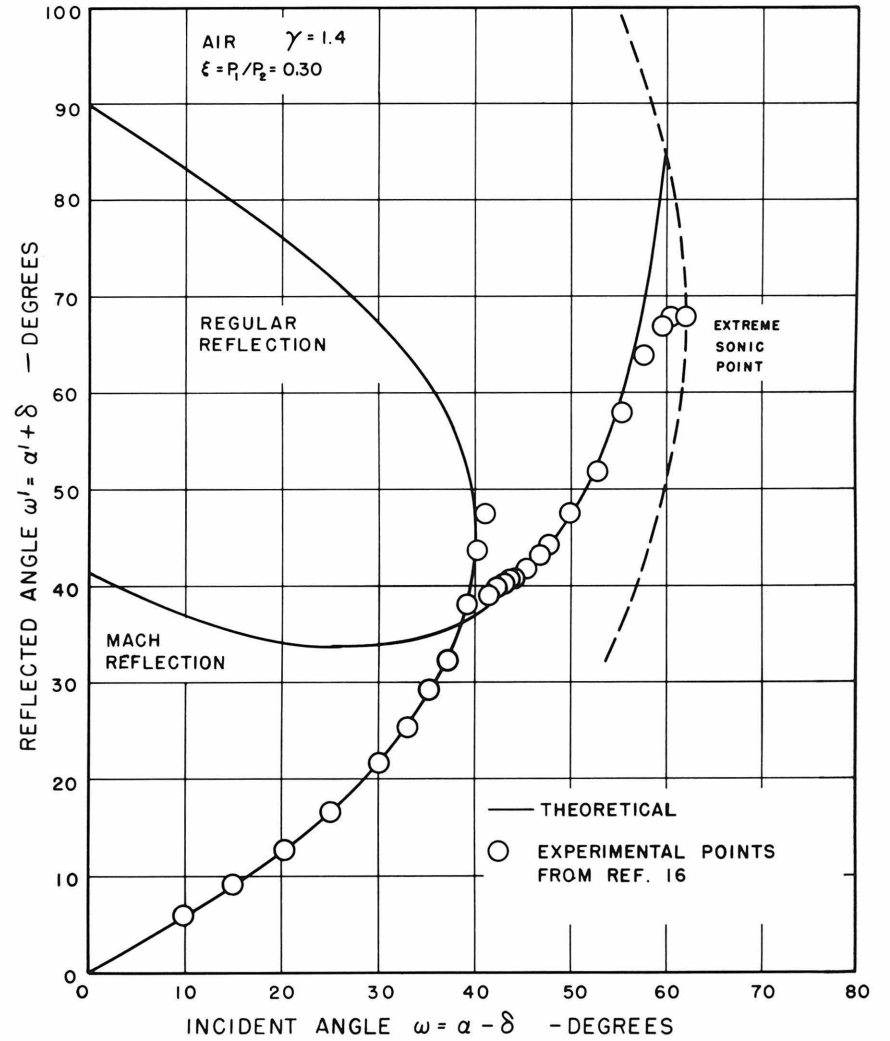
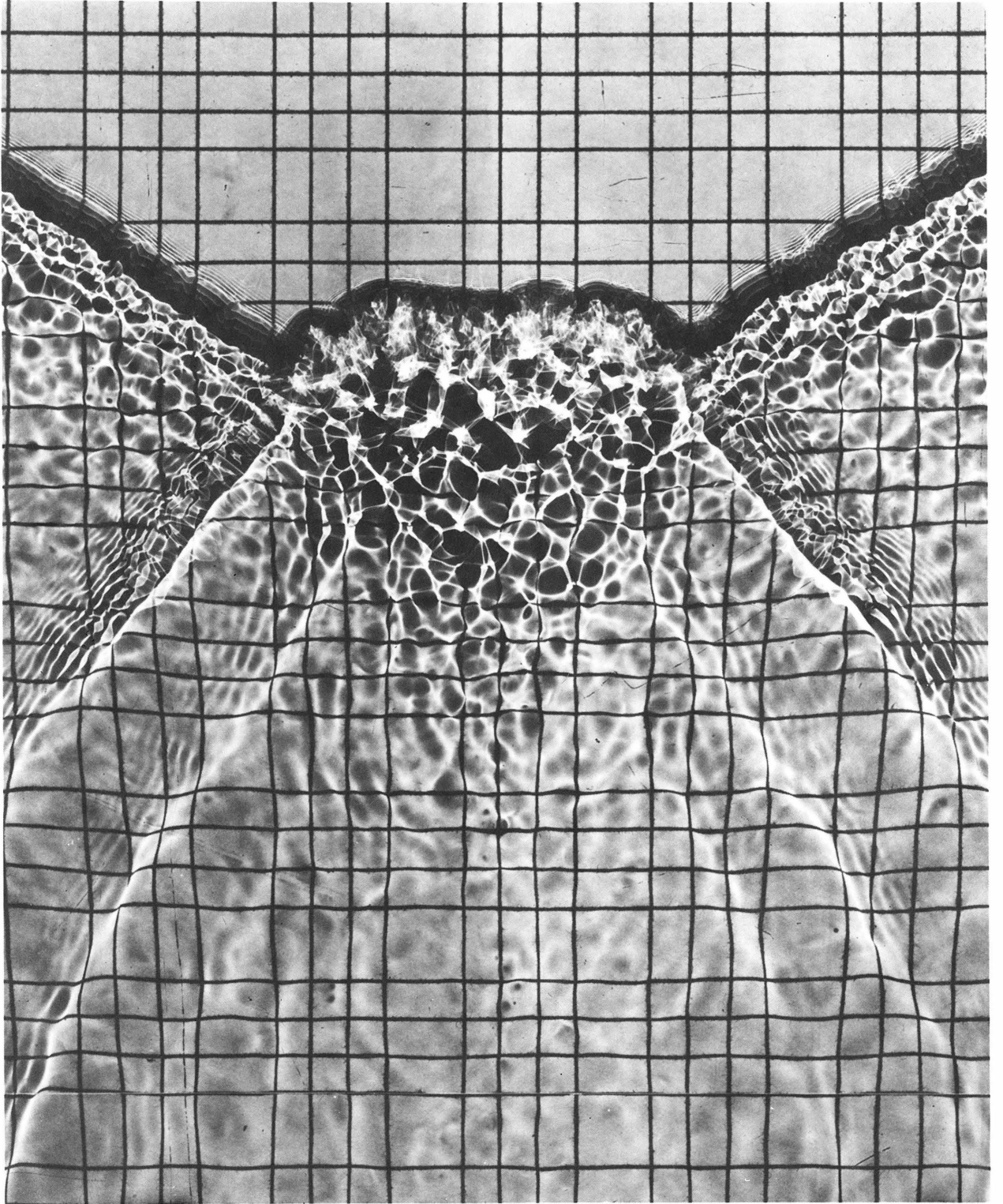Fig. 26 Reflection of Compression Shock in Air, Pressure Ratio $\xi = 0.30$.
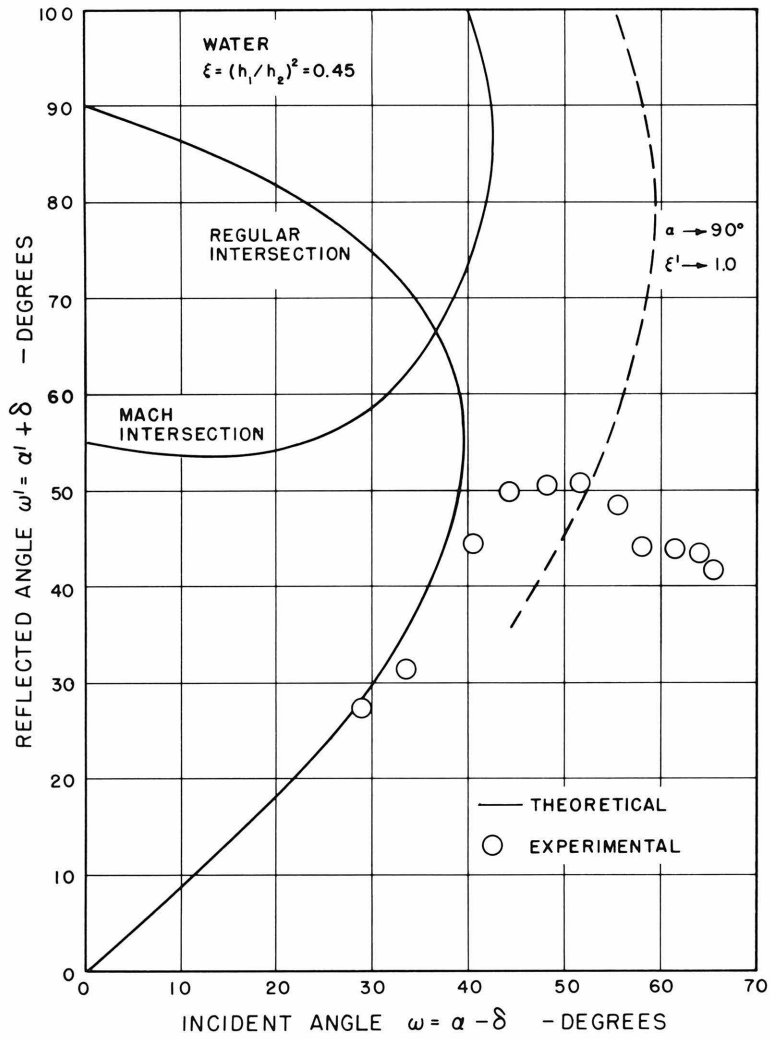
Fig. 27   Intersection of Two Equal Hydraulic Jumps of Strength ξ = 0.45.
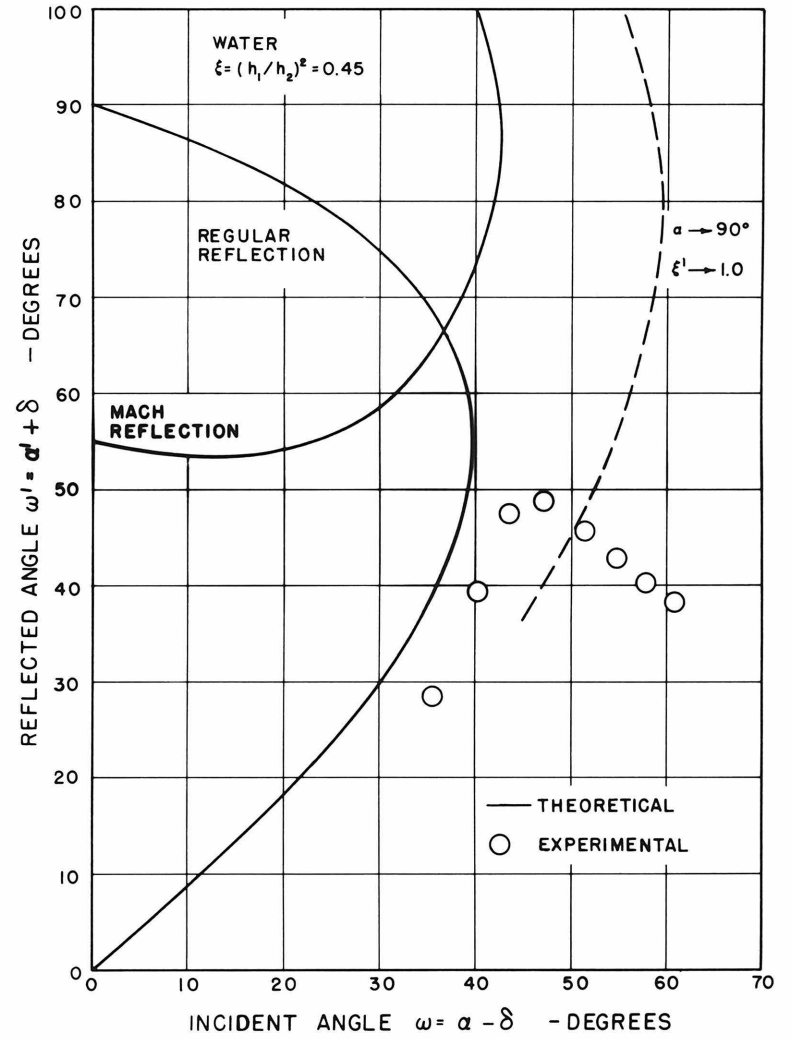
Fig. 28   Reflection from Rigid Wall of Hydraulic Jump of Strength ξ = 0.45.
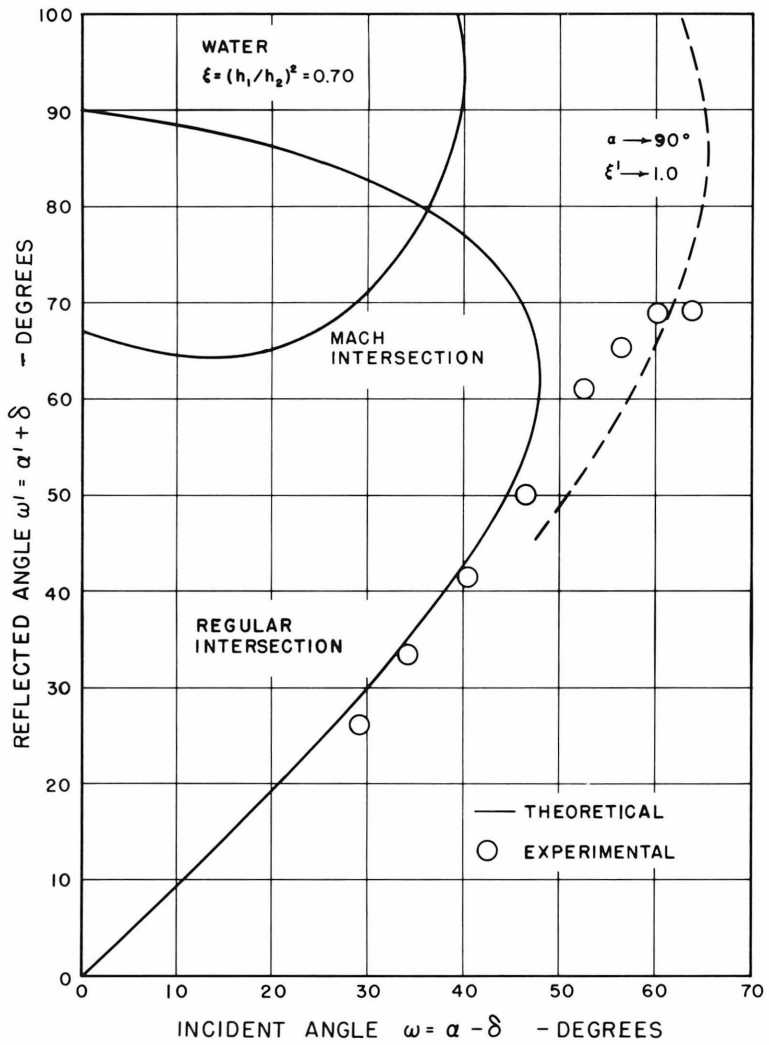
Fig. 29 Intersection of Two Equal Hydraulic Jumps of Strength $\xi = 0.70$.
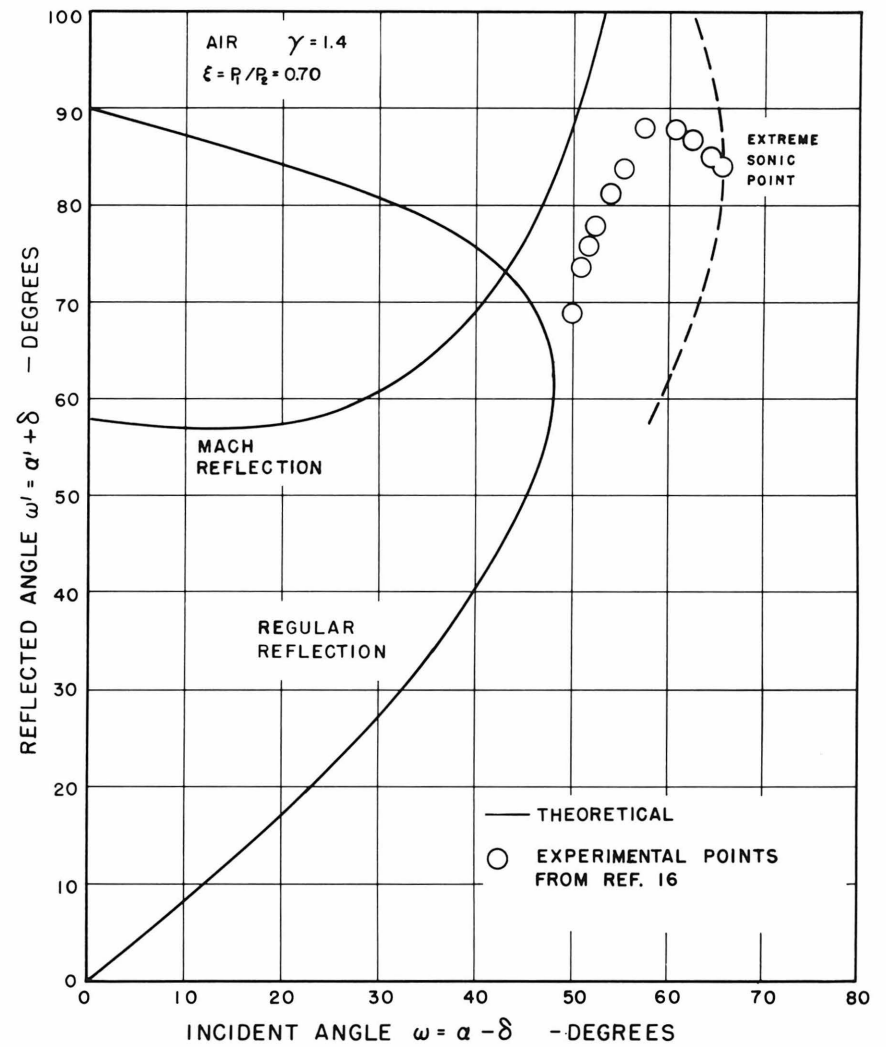
Fig. 30 Reflection of Compression Shock in Air, Pressure Ratio $\xi = 0.70$.

Fig. 31 Photogram of Hydraulic-Jump Intersection. $\xi = 0.28$, $\alpha = 56°$.
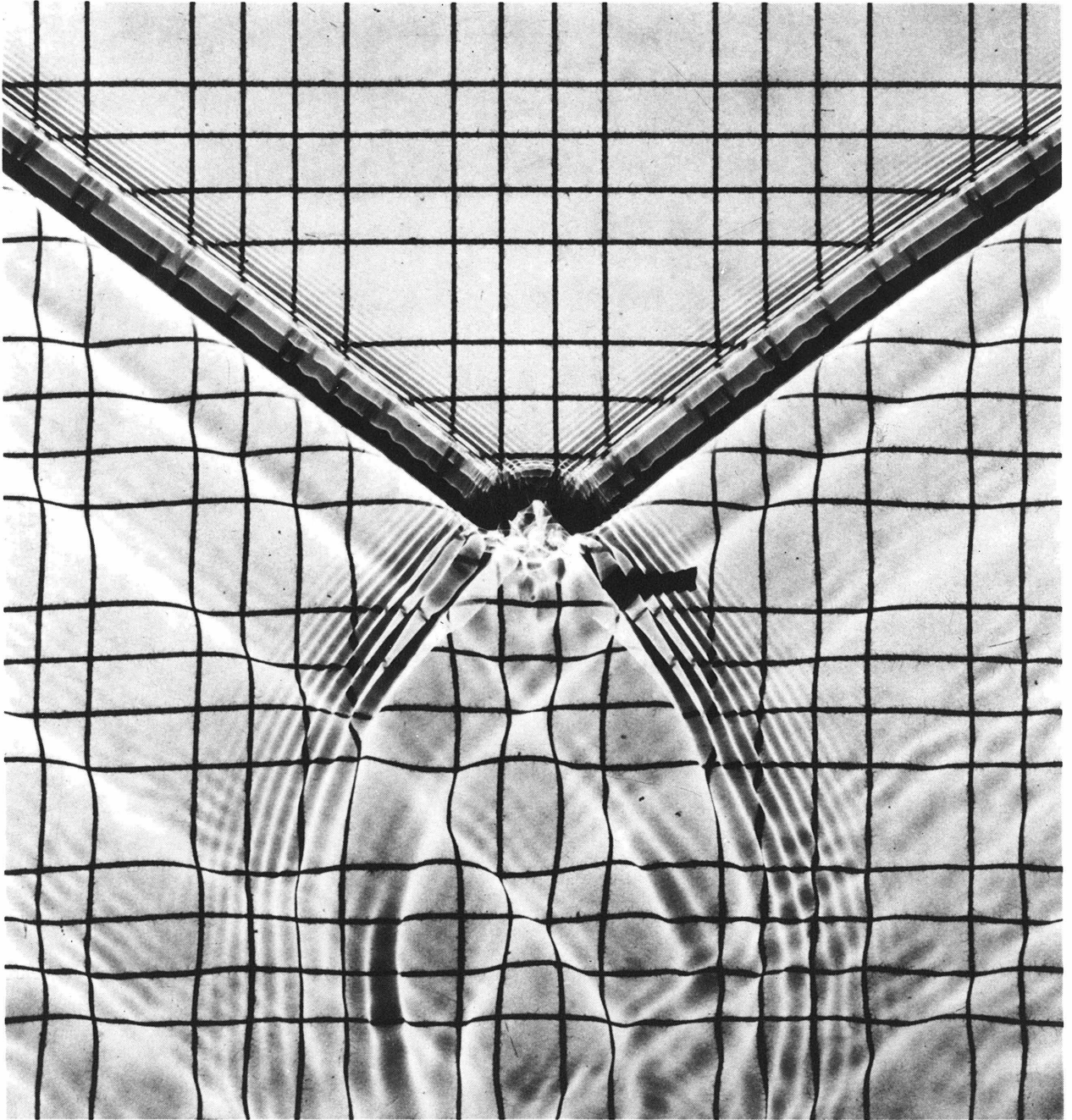
Fig. 32 Photogram of Hydraulic-Jump Intersection.   ξ = 0.45, α = 56°.
0.45 Second after Beginning of Interaction.
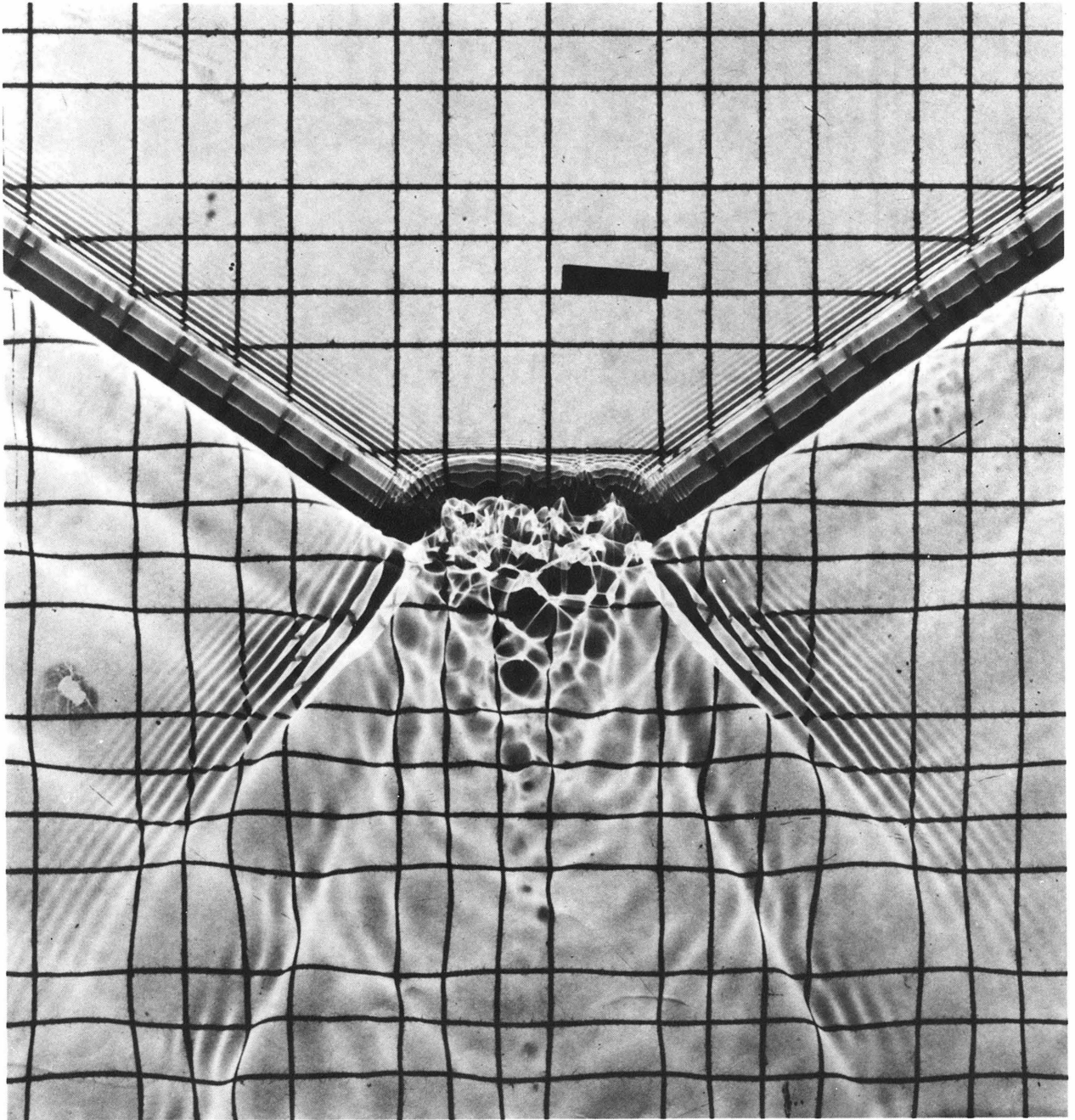
Fig. 33 Photogram of Hydraulic-Jump Intersection. $\xi = 0.45$, $\alpha = 56°$.
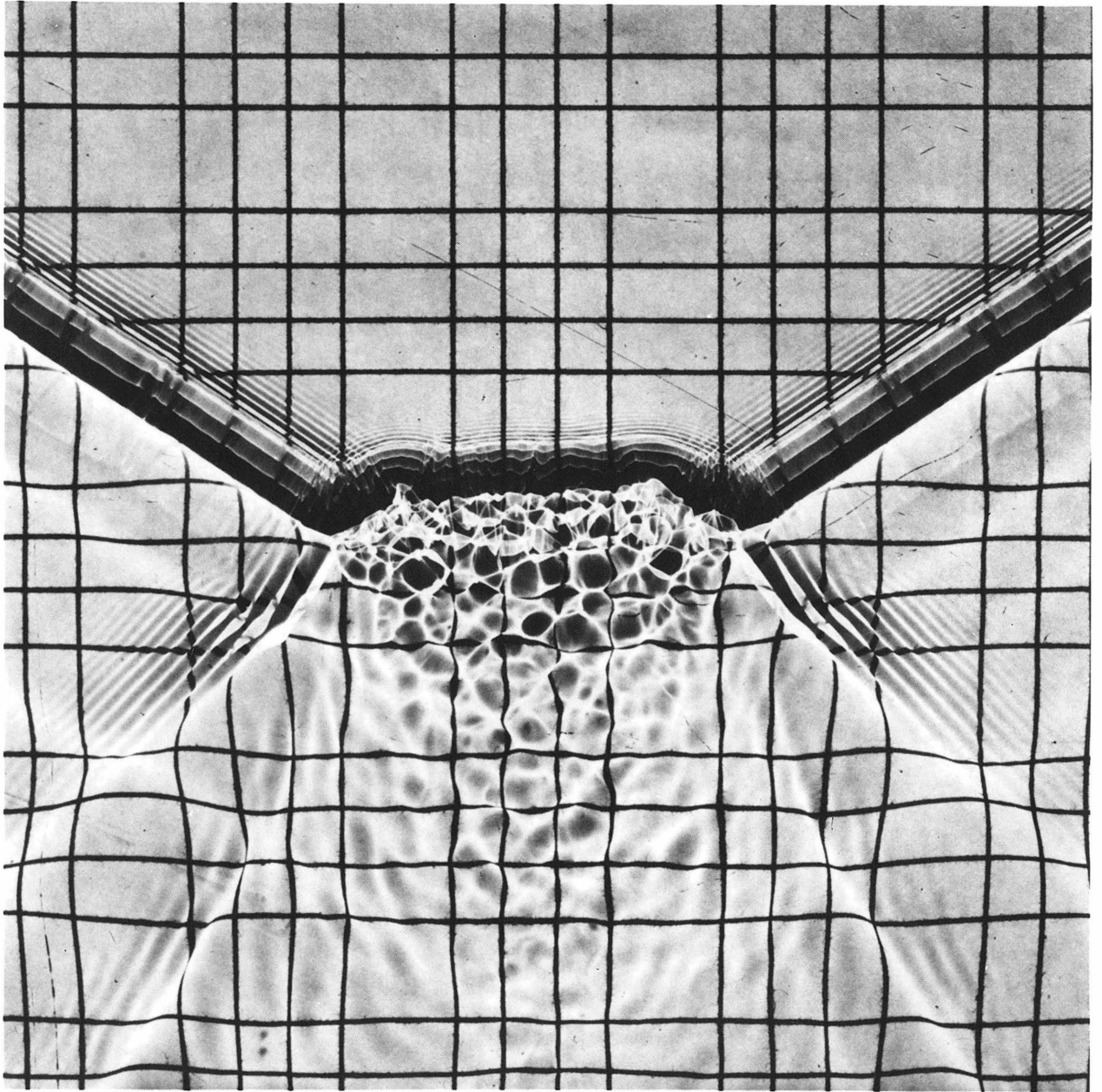0.85 Second after Beginning of Interaction.

Fig. 34 Photogram of Hydraulic-Jump Intersection. $\xi = 0.45$, $\alpha = 56°$.
1.25 Seconds after Beginning of Interaction.

Fig. 35 Photogram of Hydraulic-Jump Reflection from Wall. $\xi = 0.45$, $\alpha = 61°$.
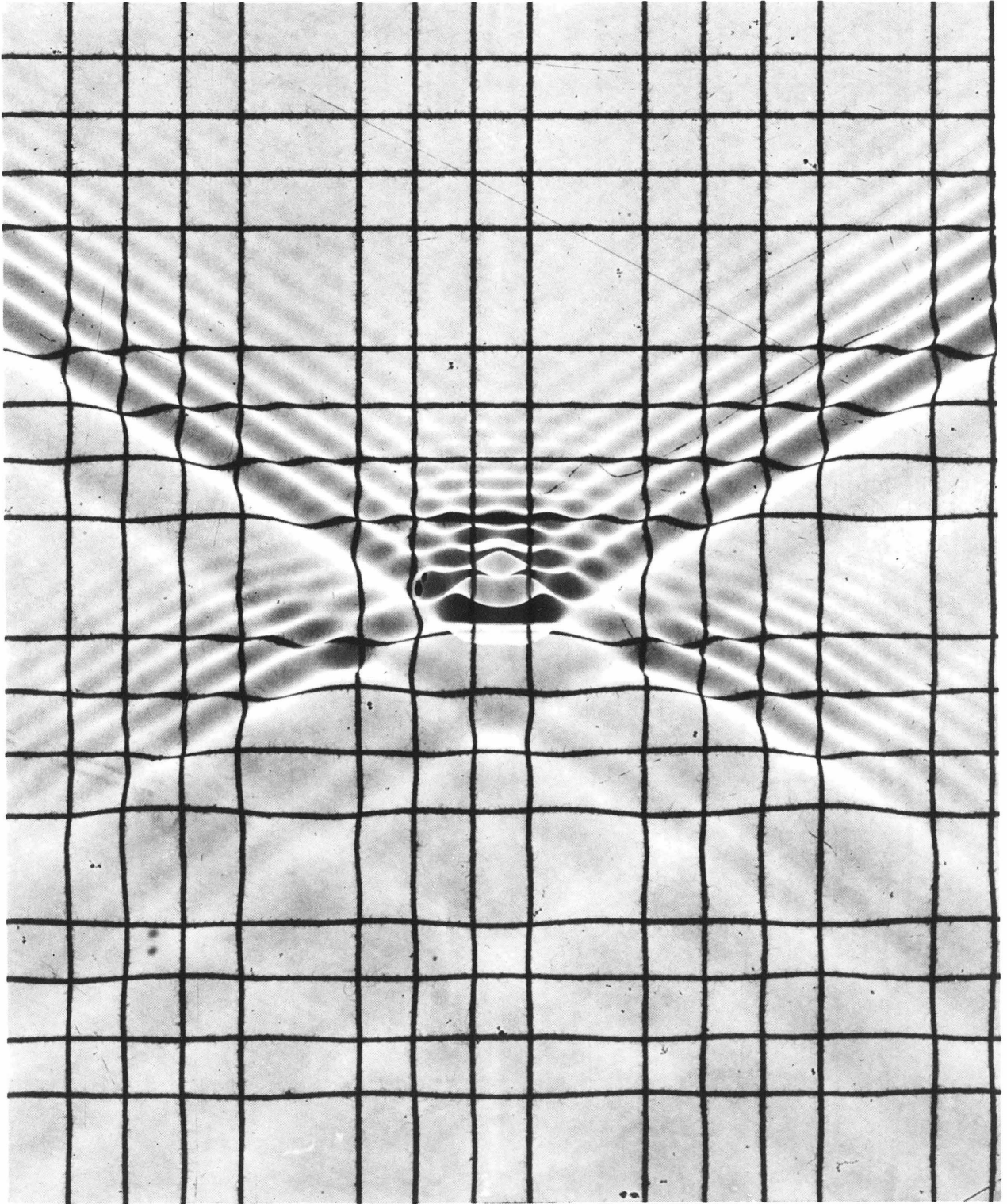
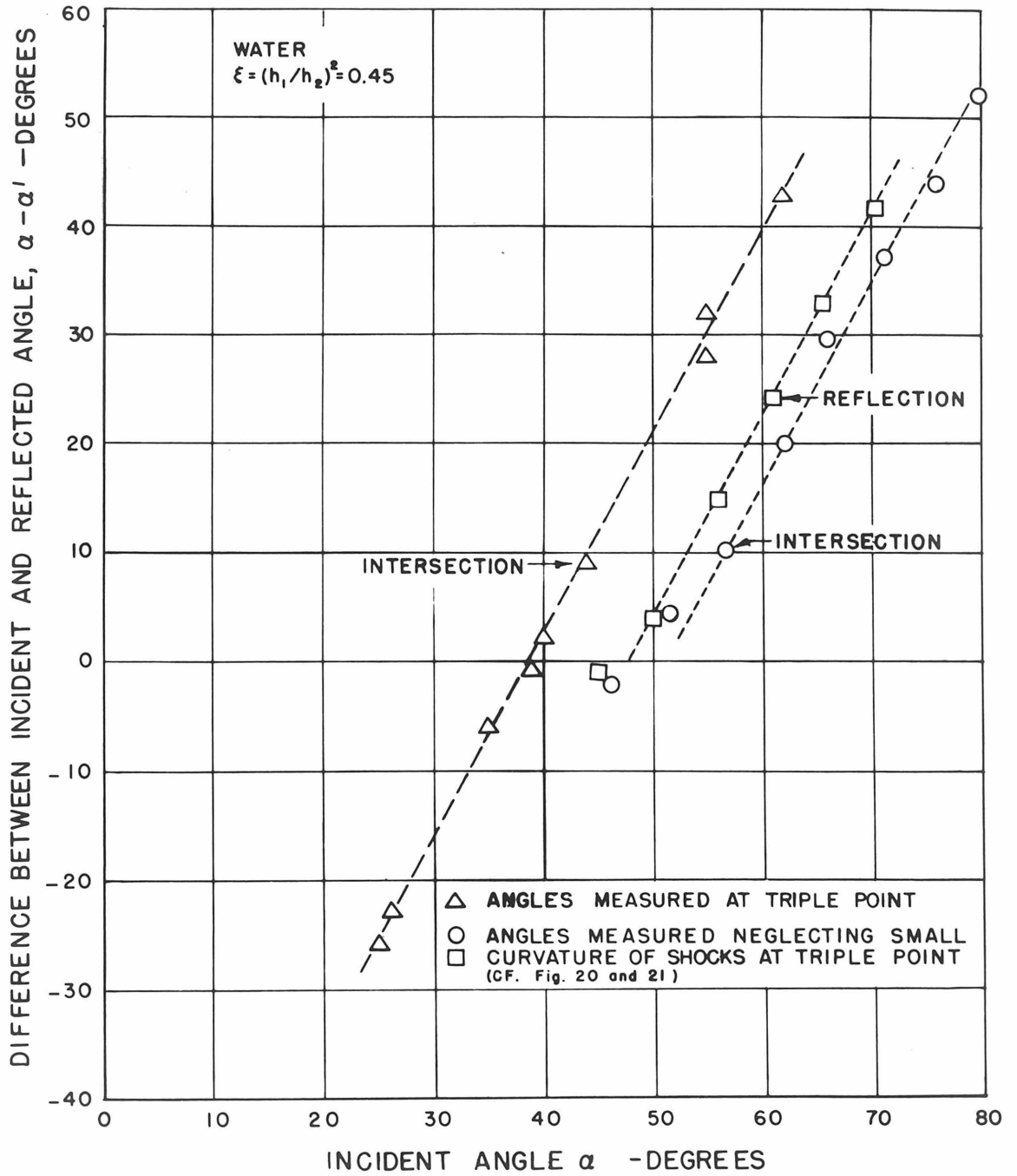Fig. 36 Photogram of Hydraulic-Jump Intersection. $\xi = 0.70$, $\alpha = 58°$.

Fig. 37 Comparison of Angles Measured at Triple Point with Angles
Measured Neglecting Small Curvature of Shocks at Triple Point